Development of a Southern Hemisphere subtropical wetland (Welsby Lagoon, south-east Queensland, Australia) through the last glacial cycle

Haidee R. Cadd[a, b *]

haidee.cadd@adelaide.edu.au

John Tibby [b, c]

john.tibby@adelaide.edu.au

Cameron Barr [b,c]

cameron.barr@adelaide.edu.au

Jonathan Tyler [a, b]

jonathan.tyler@adelaide.edu.au

Lilian Unger [g]

lilian.unger.16@ucl.ac.uk

Melanie J. Leng [d, e]

mjl@bgs.ac.uk

Jonathan Marshall [f, j]

jonathan.marshall@des.qld.gov.au

Glenn Mcgregor [f]

glenn.mcgregor@des.qld.gov.au

Richard Lewis [a, b]

richard.lewis@adelaide.edu.au

Lee J. Arnold [a, b]

lee.arnold@adelaide.edu.au

Tara Lewis [h]

lewis.taram@gmail.com

Jeff Baldock [i]

jeff.baldock@csiro.au

[a] Department of Earth Sciences, University of Adelaide, North Terrace, South Australia, 5005, Australia

[b] Sprigg Geobiology Centre, University of Adelaide, North Terrace, South Australia, 5005, Australia

[c] Department of Geography, Environment and Population, University of Adelaide, North Terrace, South Australia, 5005, Australia

[d] NERC Isotope Geosciences Facilities, British Geological Survey, Nottingham, NG12 5GG, UK

[e] Centre for Environmental Geochemistry, School of Biosciences, Sutton Bonington Campus, University of Nottingham, Loughborough, LE12 5RD, UK

[f] Queensland Department of Environment and Science, GPO Box 5079, Brisbane, Queensland, 5078, Australia

[g] Department of Geography, University College London, London, WC1E 6BT, UK

[h] School of Life and Environmental Sciences (Burwood Campus), Deakin University, Geelong, 221 Burwood Highway, Burwood, Victoria, 3125, Australia

[i] CSIRO Agriculture and Food, Locked Bag 2, Glen Osmond, 5064, South Australia, Australia

[j] Australian Rivers Institute, Griffith University, Kessels Road, Nathan, Queensland, 4111, Australia

Key words

Quaternary, Paleolimnology, Australia, MIS3, MIS4, stable isotopes, organic carbon, macrofossils, pigments, wetland

Highlights

- First description of a new, continuous sedimentary record extending from MIS5 to present from sub-tropical Australia
- An open water lacustrine environment dominated by aquatic algae and cyanobacteria occurred from approximately MIS5 to MIS2
- A transition from a lacustrine to palustrine system occurred after ca. 40 ka
- Aquatic macrophyte-dominated palustrine environment has persisted from 40 ka – present
- Sediment pigments and plant macrofossils elucidate the source of sedimentary organic material

Abstract

Continuous records of terrestrial environmental and climatic variability that extend beyond the Last Glacial Maximum (LGM) in Australia are rare. Furthermore, where long records do exist, interpretations of climate and ecological change can be hampered by marked changes in sedimentary environment which, in turn, affect the taphonomy of palaeoecological remains. As a consequence, in order to determine how wetland systems responded to climatic and environmental changes, we first need to understand how their depositional environment changed through time. Here we document the development of freshwater Welsby Lagoon, south-east Queensland, from a

12.7 m sediment sequence with a basal age of ca. 130,000 years. We present a variety of proxies reflecting change within the wetland. Carbon and nitrogen concentrations and carbon and nitrogen isotope ratios are used to infer the source of organic matter. However, the nitrogen limited nature of the catchment soils and presence of the colonial algae *Botryococcus* meant that organic material with C:N ≥20 is likely to be derived from autochthonous sources rather than terrestrial sources. A combination of photosynthetic pigments, plant macrofossils, aquatic pollen and sedimentary lignin was used to identify the sources of organic matter and the changing nature of this wetland. Since its formation, Welsby Lagoon has undergone a progressive change from an open-water, algae and cyanobacteria dominated, freshwater lacustrine system, to an aquatic macrophyte-dominated palustrine swamp after ca. 40 ka. It did not revert to lacustrine conditions during the Holocene, despite what is widely viewed as an increase in the regional moisture balance, most likely due to continual infilling of the wetland with sediment. With so few records of terrestrial change throughout MIS3 and MIS4, adequately understanding the development of sites like Welsby Lagoon is imperative to advancing our knowledge of this important environmental and cultural period in Australia's history, which encompasses events such as the extinction of megafauna and human colonisation of the continent.

1. Introduction

The last glacial cycle (from ca. 123,000 years before present; 123 ka) is a period of substantial environmental and cultural importance in Australia, encompassing the arrival of humans and the mass extinction of the Australian megafauna (Clarkson et al., 2017; Hamm et al., 2016; Roberts et al., 2001). The main terrestrial environmental and climate information for this period originate from the interpretation of proxies preserved in wetland sediments. However, the scarcity of continuous wetland sedimentary sequences extending beyond the Last Glacial Maximum (LGM; previously defined as 22–18 ka, Reeves et al., 2013), through MIS3 (57–29 ka) and MIS4 (71–57 ka), hampers

efforts to robustly investigate environmental and climatic changes. The majority of Australian sedimentary records of substantial antiquity suffer from depositional hiatuses or sedimentary deflation, commonly during the period of cold and arid climates characteristic of the LGM (Black et al., 2006; D'Costa et al., 1993; Harle et al., 2002; Longmore, 1997; Singh et al., 1981). Thus, spatially diverse interpretations of continental climate and Australian landscape change are lacking during the important time periods of MIS3 and MIS4 (Turney et al., 2006).

Welsby Lagoon provides a regionally important sedimentary record of changes in sub-tropical, eastern Australia during MIS3 and MIS4. Optically stimulated luminescence (OSL) ages from the basal sands of Welsby Lagoon indicate that the wetland formed during MIS5, with a basal age of ca. 130 ka (Tibby et al., 2017). The two other continuous wetland sedimentary sequences that extend through MIS3 and MIS4 (Figure 1), Caledonia Fen in the cool-temperate south (Kershaw et al., 2007b) and Lynch's Crater in the wet tropics (Kershaw et al., 2007a), have become the focus of a substantial number of studies (e.g. Johnson et al., 2016; Kershaw et al., 2007a, 2007b; Rule et al., 2012; Turney et al., 2004). These spatially isolated records provide the basis for many interpretations of terrestrial climate and environmental change for continental Australia. However, as highlighted by Reeves et al. (2013a), Australian climate variability during the last glacial period was spatially complex. The wide diversity of topography, large latitudinal range, extensive low-relief interior and fringing mountainous areas, has led to asynchronous, and often contradictory, responses from wetland, vegetation and ocean records. Welsby Lagoon is a lowland, sub-tropical site that fills a large spatial gap between the previously documented continuous terrestrial MIS4 and MIS3 records from tropical and temperate eastern Australia (Figure 1).

Understanding the depositional nature of wetland sedimentary sequences is a fundamental requirement for their use in robust reconstructions of external environmental and climatic conditions (Birks and Birks, 2006). Furthermore, knowledge of the origin and fate of organic matter is essential for robust palaeoclimate interpretations based on organic proxies. Sedimentary organic

matter in wetlands may be derived from terrestrial production within their catchments or be produced by autotrophs within wetlands. Autochthonous primary producers in wetlands typically consist of algae and cyanobacteria, as phytoplankton, periphyton or metaphyton and submerged, floating or emergent vascular macrophytes (Finlay and Kendall, 2008). In macrophyte-dominated wetlands, phytoplankton production is typically low, and the dominant source of sedimented organic matter is macrophytes (Blindow, 1992). The importance of emergent macrophytes diminishes with increasing wetland water depth, such that in deep lakes, primary production and hence organic matter deposition, tends to be dominated by unicellular photoautotrophs (Schlesinger and Bernhardt, 2013). These varying sources of organic matter are charactered by different concentrations and isotopic ratios of carbon and nitrogen (Meyers and Teranes, 2001).

In order to understand the history of wetland formation and variability in the sources of organic matter at Welsby Lagoon, we analysed carbon and nitrogen isotope ratios ($\delta^{13}C$ and $\delta^{15}N$) of organic matter and total organic carbon (TOC), total nitrogen (TN), macrofossil remains, autotroph pigments, sediment lignin content and pollen composition categorised into plant habitat from a 12.7 m sediment core. This multi-proxy approach provides a reconstruction of the depositional environment of Welsby Lagoon from which we infer its evolving nature, particularly its progression from a lacustrine to palustrine wetland. This foundation study provides vital information to support future research into the climate and environmental history of this region.

2. Regional Setting

North Stradbroke Island (NSI; 27°27’S, 153°28’E), south-eastern Queensland, is situated in the sub-tropical climate zone of south-eastern Australia (Figure 1A). The ocean proximity moderates temperatures, with the island experiencing warm, humid summers (mean 26°C) and mild, dry winters (mean 19°C) (BOM, 2018). The majority of annual precipitation (1500 mm) occurs during

Austral summer and autumn months, with only 15% of rainfall occurring from July to October (BOM, 2018).

The key synoptic drivers of southeast Queensland rainfall variability on annual timescales are the south-easterly trade winds, cut-off lows and extra-tropical cyclones. Regional climate is modulated on inter-annual to decadal timescales by the Inter-Tropical Convergence Zone (ITCZ), the El Niño-Southern Oscillation (ENSO) and the Inter-decadal Pacific Oscillation (IPO) (Barr et al., 2017; Moss et al., 2013 and references therein).

NSI is part of the larger regional Cooloola sand mass and is the second largest sand island in the world (285 km^2; Figure 1B). NSI last became isolated from mainland Australia by the flooding of Moreton Bay during the mid-Holocene, ca. 6000 years ago (Pye, 1993). Topographically, NSI is, for the most part, composed of a series of north-west to south-east orientated parabolic sand dunes, although Welsby Lagoon is bounded by a north – south oriented dune on the western side (Figure 1b). The Cooloola sand mass consists of a series of stabilised sand dunes formed over a number of dune-building phases from ca. 500 ka. The dunes were formed predominantly during glacial periods from the aeolian transport of continental and exposed marine sands (Lees, 2006; Miot da Silva and Shulmeister, 2016; Walker et al., 1981).

Soils on the quartz-rich sand dunes show progressive development with age, with the depth of podzol development varying in relation to dune age (Thompson, 1981). The low-nutrient capital of the quartz-dominated dunes results in relatively low soil productivity with low soil carbon contents (<2% C) (Chen et al., 2015; Stephens and Sharp, 2009; Walker et al., 1981). Dry sclerophyll forest, Casuarinaceae woodland and heath communities dominate the majority of the island, with mangrove forests found on the coastal fringes of the western side. Rainforest vegetation is restricted to a single patch on the north-west side of the island at Myora Springs (Moss et al., 2011; Stephens and Sharp, 2009).

On NSI, precipitation percolates rapidly through the sand regolith into a predominantly subterraneous, regional, freshwater aquifer (Leach, 2011). Freshwater springs and groundwater-fed lakes and wetlands occur mostly along the coastal fringe, forming where surface topography intersects the regional aquifer. The regional groundwater-regulated wetlands of NSI demonstrate remarkable stability and resilience to environmental perturbations such as fire and drought (Barr et al., 2013; Mettam et al., 2011; Specht and Stubbs, 2011; Tibby et al., 2017). Other wetlands are associated with perched aquifers that occur across the island where indurating layers of organic and/or inorganic material have developed in dune hollows (Timms, 1986). Perched wetlands can occur high above the regional aquifer, while others have developed at lower altitudes due to interactions between the perched and regional aquifers (Leach, 2011). Many NSI freshwater wetlands are palustrine, waterlogged, oligotrophic environments, dominated by sedges *Baumea* spp., *Gahnia sieberiana*, *Lepironia articulata* and *Baloskion pallens* (syn. *Restio pallens*) and open *Melaleuca quinquenervia* forest (Marshall and McGregor, 2011).

Today Welsby Lagoon (27°26’12’’S, 153°26’56’’E; 29 m.a.s.l; Figure 1C, 1D) is a perched, palustrine wetland, with a variable water depth of 0 – 1.5 m. During periods when there is no surface water present, the peaty organic sediments remain waterlogged close to the surface by the perched aquifer. Welsby Lagoon has an internally draining catchment of 5.38 km^2 (~2% of the island) and is hydrologically closed with no fluvial input. The wetland water is generally well-mixed, acidic (pH 4.3 – 6.8), soft (hardness as $CaCO_3$ 15 mg/l), nutrient deficient, and fresh (37.3 – 50 µS/cm), with very low turbidity (<2 NTU) and strongly tannin-stained waters (true colour 1370 Hazen units) (Queensland Government, unpublished data). The wetland surface is dominated by emergent sedges and reeds (*Baumea* spp. being dominant), while fringing terrestrial vegetation is dominated by Eucalypt woodland with a predominantly heathy understory of *Banksia* and Casuarinaceae (Moss et al., 2013).

3. Methods

3.1 Sediment coring

The thickest sedimentary sequence, and hence the location of core collection, was identified by a systematic sediment probing survey (Figure 1C, D). Coring was undertaken in approximately 0.5 m of water depth from a Kawhaw coring platform. Sediments were extracted as two, 0.5 m offset, parallel cores (WL15-1 and WL15-2) extending to 12.78 m and 12.72 m depth respectively. In this study only WL15-2 is discussed. The coring process minimised sediment exposure to light by using black PVC tubing coupled to a modified Bolivia corer (Myrbo and Wright, 2008). Once raised, the 1 m core sections were wrapped in black plastic to maintain the integrity of the natural luminescence signal for OSL dating. Core sections remained wrapped and sealed until being split under filtered and subdued red LED light conditions at the University of Adelaide.

3.2 Single-grain Optically Stimulated Luminescence (OSL) dating

Two 20 cm sediment samples from the WL15-2 core were dated using optically stimulated luminescence (OSL) at the University of Adelaide. OSL dating of Welsby Lagoon basal sands has previously been reported by Tibby et al. (2017). All sample extraction was conducted under filtered and subdued red LED lighting. Approximately 30 g of bulk sediment (dry weight) was retained from each sample for dose rate determination. Water and bulk density analysis was conducted on sediment samples collected at 10 cm intervals through the 12.7 m core sequence.

Preparations for equivalent dose (D_e) estimation on refined quartz fractions (180–250 µm) were conducted using standard procedures outlined in Aitken (1998), including a 48% hydrofluoric acid etch (40 minutes). Single-grain D_e measurements were made using the instrumentation and experimental procedures described by Arnold et al. (2016, 2013). Single-grain analysis was performed using a Risø TL/OSL DA-20 reader equipped with an EMI9235QA photomultiplier tube, a mounted $^{90}Sr/^{90}Y$ β source for irradiation, and a 10 mW Nd:YVO_4 single-grain laser attachment emitting at 532 nm.

Individual D_e measurements were determined using the single-grain SAR protocol (Murray and Wintle, 2000; Table S1) and D_e values were only accepted for burial dose evaluation if they satisfied a series of routine quality assurance criteria (Arnold et al., 2007; Table S2). The final burial dose estimates of samples WL15-2(3) and WL15-2(6) have been calculated using the four-parameter unlogged minimum age model (MAM-4UL; Arnold et al., 2009) and the central age model (CAM; Galbraith et al., 1999), respectively (see Supplementary Information for further details).

The sedimentological components of the environmental dose rate were calculated using a combination of inductively coupled plasma mass spectrometry (ICP-MS) and inductively coupled plasma optical emission spectrometry (ICP-OES). Elemental concentrations were converted to beta and gamma dose rates using the conversion factors of Guérin et al. (2011), with allowances for beta-dose attenuation and moisture content (Mejdahl, 1979; Table 1). The cosmic ray contribution to the total environmental dose rate was determined using the approach of Prescott and Hutton (1994), assuming a steady post-depositional overburden accumulation and a constant lake depth (equivalent to present-day conditions).

3.3 Geochemical analysis

Total organic carbon (TOC) and total nitrogen (TN) concentrations, carbon and nitrogen isotope ratios ($^{13}C/^{12}C$ and $^{15}N/^{14}N$ respectively) were determined from fifty sub-samples throughout the Welsby Lagoon core. Approximately 2 cm^3 of bulk sediment was freeze dried and ground to a homogeneous consistency using a Retsch ball mill prior to analysis. Samples were combusted in a EuroVector EuroEA elemental analyser, in-line with a Nu Instruments Nu Horizon continuous flow Isotope Ratio Mass Spectrometer at the University of Adelaide. Samples were calibrated against internal glycine, glutamic acid and triphenylamine standards through USGS40, USGS41, IAEA CH6, NBS22 and NBS24 for $^{13}C/^{12}C$ and IAEAN1, IAEAN2, IAEANO3, USGS25, USGS32, USGS40 and USGS41 for $^{15}N/^{14}N$. All carbon and nitrogen isotope ratios reported here are expressed on the delta scale ($\delta^{13}C$ and $\delta^{15}N$) to per mille (‰) relative to VPDB and AIR, respectively. Carbon to nitrogen ratios

(C:N) are expressed as weight ratios. Analytical precision for replicate measurement of standards was ±0.06‰. Standards were used to calculate a drift and peak size correction that was then applied to sediment samples.

Constrained incremental sum of squares (CONISS) was conducted in the rioja package (Juggins, 2015) in R (R Core Team, 2017) on organic geochemical data (TOC, $\delta^{13}C$, $\delta^{15}N$, C:N) to determine major groupings within the sediment core (Figure S3).

Modern algae and cyanobacteria (herein referred to as algae), emergent macrophyte, terrestrial vegetation and soil samples were collected from NSI in February 2017 (Table S3). Phytoplankton was collected by towing a 20 cm diameter plankton net with a 10 µm mesh at 0.3 m from the surface of the lake for approximately 3 minutes. Mats, crusts and other epiphytic and metaphytic algal material was collected by hand. All samples were kept chilled until observed in the laboratory. Live material was examined using bright-field, phase contrast, and differential interference contrast illumination systems with an Olympus BX53 compound microscope to a maximum magnification of 1000x. Terrestrial vegetation samples consisted of leaves and fine stem material. Emergent aquatic samples are an average of measurements taken from the tip, stem and root of each plant. Samples were freeze-dried and finely ground before being transported for analysis at the British Geological Survey. For the modern samples, $\delta^{13}C$, $\delta^{15}N$ and TOC and TN were analysed by combustion via an online Costech ECS4010 Elemental Analyser and evolved gas was transferred to a VG TripleTrap and Optima dual-inlet mass spectrometer. Samples were calibrated against in house standards (BROC and SOIL) through NBS18, NBS-19 and NBS22. Analytical precision for replicate measurement of standards was <0.1‰.

3.4 Sediment Nuclear Magnetic Resonance (NMR)

The relative proportion of lignin in sediment was estimated using solid-state ^{13}C nuclear magnetic resonance (NMR) spectroscopy on the same 50 samples analysed for stable isotopes. All spectra were acquired at the CSIRO Waite campus on a Bruker 200 Avance spectrometer equipped with a

4.7 T wide-bore superconducting magnet operating at a resonance frequency of 50.33 MHz. Weighed samples (150-600 mg) were packed into 7 mm diameter zirconia rotors with Kel-F end caps and spun at 5 kHz. Chemical shift values were calibrated to the methyl resonance of hexamethylbenzene at 17.36 ppm and a 50 Hz Lorentzian line broadening was applied. A cross polarisation (CP) pulse sequence as used with a delay between pulses set to the longer of 1 s or five times sample specific T1H values determined by inversion recovery analysis. A 3.2 µs and 195 w 90° pulse with a 1 ms contact time was used, with between 10,000 and 20,000 transient collected for each sample. All spectral processing was completed using the Bruker TopSpin 3.2 software. After phasing and baseline corrections were applied, the absolute NMR signal intensities acquired for each sample were divided by the number of transients collected and corrected for the empty rotor background signal intensity. The resultant spectral intensities were integrated over a series of chemical shift limits and used to estimate the lignin content of the samples according to the calculations described by Baldock et al (2013).

3.5 Palynology

Pollen samples were processed using a modified version of the standard protocols outlined in Faegri and Iverson (1989). Sixty x 0.5 cm^3 sediment samples were taken at ~20 cm intervals along the length of the core. A total of 250 grains of terrestrial origin (excluding fern spores) form the base pollen sum. Percentages of aquatic taxa are based on a super-sum inclusive of both terrestrial and aquatic taxa. Terrestrial taxa are grouped according to morphology and habitat types.

3.6 Macrofossils

Macrofossil analysis was undertaken on 19 samples, with sampling effort focussed on the depths from 380 – 790 cm. Macrofossil samples were processed using the methods outlined in Birks (2002). Sediment (30 cm^3, 3 cm of core depth) was extracted for each sample and measured using volume displacement in 50 mL of water. Samples were gently rinsed through nested sieves to separate the >250 µm and >125 µm size fractions. All material retained in the 250 µm sieve was examined and 10

mL sub-samples of the >125 µm fraction were examined. Material was identified using a combination of online and print identification guides, modern samples and a macrofossil reference collection and database (Lewis, 2012). The abundance of material of unknown taxonomic origin (dominated by stem material) was estimated using a point count method (after Clark, 1982). In this method, 5 ml aliquots of the >250 µm material were taken from a 200 ml suspension of material and added to a gridded petri dish with 60 intersections or "points." The number of times plant material fell on these points was then recorded and expressed as a percentage.

3.7 Sedimentary pigments

Pigments were extracted from 14 sediment samples. Pigment analysis was performed at the Queensland Government's Department of Environment and Science's Chemistry Centre laboratories using a modified HPLC method. Sediment samples (~0.4 g) were combined with 3 ml of acetone and homogenised using a ceramic mortar and pestle. An additional 2 ml of acetone was added and solution was refrigerated at -20^{o}C for 2 hours before being filtered using a 0.22 µm nylon syringe filter. Samples were dried under N_2 gas and reconstituted with 200 µl of 7 mM tetrabutyl ammonium acetate and methanol. HPLC analyses were performed on a Dionex Ultimate 3000 U-HPLC system with a Dionex DAD 3000 diode array detector. 10 µl of each sample and an intermediate standard (containing lutein, β-carotene, zeaxanthin, alloxanthin, fucoxanthin, chl α and peridinin) were injected onto a Phenomenex chromatographic system with an inline 0.2 µm filter. Pigment data was calibrated using response factors of certified mixed pigment standards. Chromatograms were integrated using Chromeleon 7.2 acquisition software with pigments identified using a combination of their retention times and absorbance spectra. Pigment concentrations are expressed as ng/g of carbon based on measured TOC. Taxonomic affinities of identified pigments were determined from Leavitt and Hodgson (2002) and Roy et al. (2011).

4. Results

The modern plant and algae samples all have $\delta^{13}C$ values consistent with those of C_3 plants (–24 to –34 ‰, Figure 2, Supplementary Table 1; Meyers and Teranes, 2001). Terrestrial plants have the lowest $\delta^{13}C$ values of all samples, from –30.4 to –31.6 ‰ (Figure 2A, 2C). Algae exhibited the largest range of $\delta^{13}C$, from –27.2 to –31.7 ‰ (mean –29.2 ‰) (Figure 2A, 2C). Emergent aquatic plants have the highest $\delta^{13}C$, from –23.1 to –29.3 ‰, however these still fall within the global C_3 plant range (Figure 2A). All modern samples (including the algae) have C:N ratios above 18. Algae samples have the lowest C:N ratios ranging from 18 to 46. All terrestrial and emergent aquatic vascular plants have C:N ratios above 40 except for *Eucalyptus* leaves, with a value of 29 (Figure 2A, 2D).

The 12.7 m sediment core recovered from Welsby Lagoon consists of highly organic, dark coloured sediment (Figure 3). CONISS, conducted on organic geochemical data (TOC, $\delta^{13}C$, C:N; Figure S3), in conjunction with lithology (i.e. changes in sediment type), was used to separate the sediment core into three phases. Three OSL and radiocarbon ages were used to infer the broad timing of major changes in sediment deposition. OSL samples WL15(2)-3 and WL15(2)-6 were analysed for this study (Table 3; Sup info Table S1, S2, Figure S1) and OSL sample GU5.1 from the basal sands of the wetland from Tibby et al., (2017). Radiocarbon ages from a core taken from the edge of Welsby Lagoon (Barr et al., 2017; Chang et al., 2015; Moss et al., 2013) were correlated to the upper sediments of the core used in this study (Supplementary Figure S2). Based on changes in sedimentology and the preliminary OSL and ^{14}C ages, we cautiously infer three main phases corresponding broadly to early marine isotope stage 5 (MIS5), MIS5 – MIS3 and MIS2 – present.

Phase 1 comprises the sediments below 1210 cm and consists of a thick sand layer at the base and intermixed sandy organic lake muds from 1266 – 1210 cm (Figure 3). The basal sands of Welsby Lagoon were OSL dated to 130 ± 15.3 ka (Tibby et al., 2017). Phase 2 occurs from 1210 – 500 cm and is comprised of homogenous, elastic, fine grained, dark organic sediments. The top 500 cm of the core is designated as phase 3 and is composed of poorly decomposed, sub-fibrous, organic sediments. Phase 1, comprising only 60 cm of the core, is represented by few analysed samples. This

section is characterised by low TOC, $\delta^{13}C$, $\delta^{15}N$ values and high C:N ratios. Phase 2 and 3 comprise the remainder of the record and are clearly distinct in their geochemical properties, with no overlap in either the $\delta^{13}C$ vs. C:N and TN vs. TOC space (Figure 2). This shift in organic composition coincides with a change in sedimentology, from fine consolidated sediments to decomposed sub-fibrous peat (Figure 3). The shift in sedimentology and organic geochemistry occurs in the middle of a drive (4.5 – 5.5 m) in the WEL15-2 core and is therefore not an artefact of coring.

TOC concentrations are high throughout the record (25.3 – 67.1 %), with a 25 % increase in TOC occurring between 530 and 485 cm. In contrast, TN concentrations are low throughout the record (0.77 – 1.72 %), with a slight long-term increasing trend. The C:N ratios are lowest and least variable in phase 2, yet are consistently above 27. The highest C:N values (46.6 – 57.1) occur between 485 and 360 cm. The proportion of lignin exhibits similar trends to the C:N ratio, with lower values (11.6 – 35.6%) in phase 2, a marked increase in values between 509 – 360 cm (43.0 – 56.7 %) and maintenance of high values from 360 – 0 cm (32.2 – 45.3 %; Figure 3). Phase 2 has the highest $\delta^{15}N$ values of 1.52 – 2.8 ‰, which declined substantially between 509 – 405 cm (–1.81 to –0.87 ‰). A brief return to positive values occurs between 380 and 320 cm (0.22 to 0.52 ‰) until a decrease in $\delta^{15}N$ values from 319 – 0 cm (–0.47 to –2.23‰; Figure 3). The $\delta^{13}C$ record exhibits an inverse relationship to $\delta^{15}N$, with the lowest values (–29.8 to –27.8 ‰) occurring in phase 2 and highest values (–27.7 to –25.9 ‰) occurring in phase 3 (Figure 3).

In contrast to the organic matter record, there is no major change in terrestrial vegetation composition at 500 cm (Figure 3). The major change in sediment lithology and geochemical data follows a slight change in pollen composition, with an increase in tree and shrub pollen at the expense of herb and grass taxa, at 680 cm. In addition, there is a reduction in rainforest pollen at 808 cm, with a shift to a more sclerophyllous and open grassland vegetation. Whilst there is no change detectable in the terrestrial pollen record, there is a steady increase in the percentage of emergent aquatic pollen from 528 cm that reaches peak values at 408 cm (Figure 4). Emergent

aquatic pollen reflects a similar pattern to the C:N and lignin data, with peak aquatic pollen between 488 and 356 cm.

Changes in macrofossil relative abundances display similarities with both the isotope and pollen data (Figure 4). The basal part of the record, from 1210 – 780 cm, is characterised by low concentrations of macrofossil remains, with those present being dominated by fern sporangia (cf. Polypodiaceae). After 750 cm, there is an increase in the percentage of overall plant macrofossil remains, as well as an increase in the presence of *Selaginella uliginosa*, a small perennial herb common in swampy locations, and *Lepironia articulata*, an emergent aquatic sedge which can grow in water depths ranging from no standing water to over 3 m (Marshall and McGregor, 2011). *S. uliginosa* is rare in the record above 625 cm. After the decline in *S. uliginosa*, there is a period of dominance by the charophyte macroalgae *Nitella* and emergent rush *Typha orientalis*. The dominance of *Nitella* is short lived and it is largely replaced at 505 cm by *L. articulata*, Casuarinaceae anthers and a variety of swamp adapted terrestrial herbs. In concert with the changes in the $\delta^{15}N$, C:N, lignin and emergent aquatic pollen records, the relative representation by terrestrial taxa declines above 380 cm. Macrofossil remains of *L. articulata* and Casuarinaceae anthers still occur in the upper portion of the record, however are present at much lower concentrations.

Sedimentary pigment concentrations are generally higher at the base of the sediment core, with the highest concentrations occurring at 1081 and 566 cm (Figure 5). Chlorophyll α is undetectable in all samples, however Chlorophyll α derivatives (Pheophytin α, Pyropheophytin α and Pheophorbide α) are present in all samples with an overall declining trend towards the top of the core (Figure 5). Carotenoid pigments are abundant in all samples, with pigments indicative of green algae (Lutein and Astaxanthin) being the most abundant in samples from 1150 – 681 cm and pigments indicative of cyanobacteria (Myxoxanthophyll, Echinenone and Zeaxanthin) and colonial cyanobacteria (Canthaxanthin) being most abundant in samples from 566 – 96 cm. Although pigment concentrations were lowest in the top part of the core, they were well above the limit of detection.

5. Discussion

The modern terrestrial, algae and emergent aquatic plant samples indicate that organic material with C:N >20 may be indicative of either lacustrine algae, emergent aquatic or terrestrial plant sources. In general, terrestrial and aquatic vascular plants contain large proportions of nitrogen poor structural carbon, such as lignin, leading to high C:N ratios. Non-vascular, unicellular algae contain minimal structural carbon and are relatively nitrogen rich due to their high protein content, leading to lower C:N ratios (Meyers and Teranes, 2001; Talbot, 2001). Modern algae samples collected from NSI have C:N ratios in excess of 18, values considered in other settings to be indicative of terrestrial plants (Figure 2; Meyers and Teranes, 2001). High C:N values have previously been reported from the colonial green alga *Botryococcus* (Heyng et al., 2012) and from algal-dominated organic matter in N-limited systems (Hecky et al., 1993; Mayr et al., 2009). High C:N ratios in *Botryococcus* result from high lipid and hydrocarbon contents (Heyng et al., 2012; Huang et al., 1999). Algal growth under N-limited conditions can result in cell material with a C:N ratio as high as 20 (Healey and Hendzel, 1980; Hecky et al., 1993; Talbot and Lærdal, 2000).

Water quality data from NSI lakes show evidence for nitrogen limitation. Brown Lake, a large perched lake, has 7 years of nutrient (N and P) monitoring data. Using the Redfield ratio of 16:1 N:P as a threshold, Brown Lake was N limited for over half the monitoring period. (Supplementary Figure S4). Soil nutrient concentrations in the Cooloola dune system show that nitrogen limitation is common on younger dunes (<130 – 170 ka), with phosphorus becoming increasingly limiting on older dunes (Chen et al., 2015). In summary, nitrogen limitation may help to explain the relatively high C:N ratios of modern North Stradbroke Island algal samples.

Nitrogen limitation is inferred during phase 2 of the sedimentary record from the high levels of astaxanthin, a pigment found in green algae in nitrogen limited waters (Lee, 2008; Roy et al., 2011; Figure 5). The presence of pigments indicative of N-fixing cyanobacteria (Myxoxanthophyll,

Echinenone, Canthaxanthin and Zeaxanthin) also contribute to the interpretation of N-limitation within the system, as these taxa have a competitive advantage during times of low nitrogen availability (Vitousek et al., 2002). Low levels of inorganic nitrogen are further indicated during phase 2 by the TOC vs. TN plot that indicates the majority of nitrogen is bound with organic carbon (Figure 2B). The intercept of the regression line at 0.05% on the TN axis suggests that at the time of deposition almost all nitrogen within the system was organically bound (Talbot, 2001). Based on the change in TOC vs. TN and the presence of N-limited green algae and cyanobacterial pigments in sediments from 500 – 1200 cm, it is very likely that Welsby Lagoon has been nitrogen limited for the entirety of is existence.

Modern samples from NSI highlight the need for caution when interpreting C:N ratios. Algal organic matter produced in N-limited waters as well as colonies of the green algae *Botryococcus* have been previously been observed to produce C:N ratios greater than 20 (Hecky et al., 1993; Heyng et al., 2012; Huang et al., 1999; Talbot and Lærdal, 2000). Based on this, and the C:N ratios of modern algal samples from NSI, we conclude that the C:N ratio indicative of allochthonous material from these systems will be ≥ 20. Therefore, the C:N ratios ≥ 20 during phase 2 are interpreted here to derive from autochthonous primary productivity, namely lacustrine algae, due to continued N-limitation within the system and/or the presence of the colonial green algae *Botryococcus* (Figure 4).

5.1 Phase 1

The basal sands from Welsby Lagoon have previously been dated with OSL, returning an age of 130 ± 15.3 ka for the initial formation of the wetland (Tibby et al., 2017). From 1260 – 1210 cm sand layers are intermixed with organic lake sediments. This section of the core extends through MIS5, but it is unlikely to be continuous, as indicated by the presence of sand layers that probably represent depositional unconformities.

5.2 Phase 2

The Welsby Lagoon record from 1210 – 500 cm is comprised of 7 m of continuous, homogenous lake muds. This section of the core, to ca. 40 ka likely represents part of MIS5, the entirety of MIS4 and the majority of MIS3. It is characterised by high organic carbon inputs, and relatively low C:N and lignin values (Figure 3). We infer that the bulk of organic carbon deposition during this time was dominated by autochthonous algal primary productivity. This interpretation is supported by low $\delta^{13}C$, low macrofossil concentrations and high concentrations of algal sedimentary pigments. Sedimentary pigments in this phase are dominated by astaxanthin, a pigment produced by green algae in nitrogen-limited environments (Figure 5). The carotenoid pigments fucoxanthin, diatoxanthin and diadinoxanthin are also found in this phase and can be derived from both diatoms and dinoflagellates (Leavitt and Hodgson, 2002; Roy et al., 2011). Low but consistent inputs of echinenone and zeaxanthin and high levels of canthaxanthin, indicate the presence of N-fixing phototrophic cyanobacteria. Combined, the autotrophic pigment composition, high TOC, low TN, low C:N, and low lignin values indicate a nutrient poor, but relatively productive, open water environment dominated by autochthonous algal organic carbon production throughout phase 2.

Sedimentary $\delta^{13}C$ generally reflects the $\delta^{13}C$ of the dominant source of organic matter entering a wetland system (Meyers and Arbor, 2001). Within the sediments of phase 2, $\delta^{13}C$ is most similar to modern algal samples from the island, though could also be derived from an approximately equal contribution of organic matter from aquatic (higher $\delta^{13}C$) and terrestrial (lower $\delta^{13}C$) vascular plant end members. However, the absence of terrestrial and emergent plant macrofossils, and low C:N and lignin values indicate that terrestrial material is unlikely to be a major contributor to sedimentary carbon, and hence that autochthonous algae is the most likely source of organic matter. During periods of enhanced algal productivity, the preferential uptake of ^{12}C depletes the carbon pool and the $\delta^{13}C$ of the dissolved inorganic carbon (DIC), and hence sedimentary carbon, becomes enriched in ^{13}C (Leng, 2006; Leng and Marshall, 2004). In addition, an increase in algal

growth rate reduces the DIC-organic carbon fractionation factor during photosynthesis, resulting in higher $\delta^{13}C$ values in the organic carbon (Laws et al., 1995). Thus, isotope changes of algal-dominated sedimentary organic material are indicative of changes in lake productivity (Mayr et al., 2009). The $\delta^{13}C$ during this phase exhibits fluctuations that are therefore likely reflecting changes algal productivity. Changes in lake productivity may reflect changes in nutrient availability or depositional processes, with an increase in nutrient supply or concentration driving an increase in $\delta^{13}C$.

The $\delta^{15}N$ of sedimentary organic matter reflects multiple biogeochemical processes, including uptake of dissolved inorganic nitrogen (DIN) by primary producers, denitrification, nitrogen fixation and organic matter degradation during sedimentation (Talbot, 2001). In N-limited systems all DIN is consumed and discrimination against ^{15}N is small, resulting in $\delta^{15}N$ of organic matter that reflects the DIN pool in which it formed (Leng, 2006). Nitrogen fixing cyanobacteria have a competitive advantage in N-limited systems, and deposit organic matter with $\delta^{15}N$ which is slightly lower than that of atmospheric N (0 to –1‰). If DIN is not fully utilised, preferential uptake of ^{14}N results in organic matter that is isotopically lighter than the substrate. The $\delta^{15}N$ values through phase 2 maintains consistent positive values (Figure 3) suggesting that isotopic discrimination is small.

Whilst the geochemical signatures of organic material implies the persistence of lacustrine conditions at Welsby Lagoon during phase 2, the macrofossil record indicates a gradual shallowing and shift to drier conditions after 825 cm (Figure 4). In addition, the decline in rainforest pollen after 800 cm implies drier conditions more broadly across the island. This progressive drying is consistent with a transition to increasingly more arid climates through MIS4 and MIS3 seen in both pollen records from eastern Australia (Kershaw et al., 2007b, 2007a; Kershaw and Nanson, 1993; Moss and Kershaw, 2000) and fluvial archives that exhibit reduced activity across central and northern Australia (Chen and Barton, 1991; Cohen et al., 2012; Cohen and Jansen, 2015; Nanson et al., 2008).

5.3 Late MIS3 and LGM

The second phase of the record commences at 500 cm (ca. 40 ka) with a large and permanent shift in both the amount and isotope signature of sedimentary carbon, along with a number of other of proxies ($\delta^{15}N$, C:N, lignin, autotroph pigments and macrofossil composition; Figure 3 & 4). This distinct change is not apparent in the terrestrial vegetation, suggesting that the $\delta^{13}C$, $\delta^{15}N$, TOC, C:N, lignin, autotroph pigments and macrofossil composition records primarily reflect within-wetland conditions.

The higher organic carbon input from 500 cm to present could have been driven by a reduction in water depth at the centre of the basin that prompted an increase in the dominance of emergent aquatic vegetation (Figure 3 & 4). An increase in rooted macrophytes leads to higher rates of carbon burial in sediments, as well high C:N and lignin concentrations (Saunders et al., 2014). In macrophyte dominated wetlands, the primary source of sedimentary organic matter is emergent aquatic plants that typically possess higher $\delta^{13}C$ than algae because they utilise both dissolved and atmospheric CO_2 (Gu et al., 1996). This is also the case for the modern samples from NSI that show that emergent aquatic plants tend to have higher $\delta^{13}C$ than algae (Figure 2A). A transition to an emergent macrophyte dominated wetland also explains the shift to lower $\delta^{15}N$ values. Rooted macrophytes often have negative $\delta^{15}N$ values due to their ability to utilise nitrogen both from the water column and recycled from decomposing sediments (Barko et al., 1991; Chang et al., 2009; Drew et al., 2008).

The transition to an emergent macrophyte dominated system is also reflected in the macrofossil and aquatic pollen records, with an increase in aquatic plant remains and aquatic pollen occurring above 505 and 460 cm respectively (Figure 5). The decrease in total concentration of sedimentary pigments from 500 cm could be a result of reduced algal productivity, dilution by pigment-poor lithic material and/or shallowing water. Photosynthetic pigments are highly labile and degradation can occur with increases in light, oxygen and temperature (Sanger, 1988), conditions associated with shallowing water.

The transition of Welsby Lagoon from a lake to an emergent macrophyte dominated swamp may have resulted from a shift in climate or by crossing a threshold of basin infilling, or a combination of the two. A return to deeper water following this transition is indicative of a climate control, rather than a threshold of basin infilling being reached. A hypothesised hydrological driver, is supported by proxy changes (i.e. reduction in lignin, C:N, macrophyte macrofossils and pollen and $\delta^{15}N$) after 380 cm (ca. 18 ka), indicating a return to less terrestrial, deeper water conditions similar to phase 2 of the record. The timing of this increase in moisture is consistent with locally inferred wetter conditions (Barr et al., 2017; Moss et al., 2013; Petherick et al., 2017), as well as broader regional conditions that indicate increased precipitation during the early deglacial (18 – 15 ka; Kershaw et al., 2007b; Petherick et al., 2008, 2011, Reeves et al., 2013a, 2013b).

The desiccation of sediments from an edge core from of Welsby Lagoon (Figure 1C) at ca. 22 ka (Barr et al., 2017; Chang et al., 2015) indicates that the standing water of the wetland had contracted towards the middle of the site during this time. The proxy records (TOC, $\delta^{13}C$, lignin, C:N, macrofossils, pollen and $\delta^{15}N$) suggest a shallowing of the wetland between 500 – 360 cm, however continued deposition of organic wetland sediments at the centre of the lagoon indicates there was still sufficient moisture to sustain the Welsby Lagoon wetland. In addition to the positive moisture balance inferred from the aquatic proxies, the terrestrial pollen record suggests that arboreal vegetation persisted throughout this period, in contrast to the dominance of grass and herb vegetation in other parts of Australia (Kershaw et al., 2007b, 2007a; Van Der Kaars and De Deckker, 2002). The absence of sand layers and the persistence of arboreal pollen taxa indicates that the landscape of NSI was relatively stable from MIS5 to present. An island-wide landscape stability is supported by pollen records from Native Companion Lagoon and Tortoise Lagoon, and the absence of sand layers in other NSI wetland records (Barr et al., 2017; Moss et al., 2013; Tibby et al., 2017). There are three potential hypotheses that could lead to the persistence of a shallow wetland during the LGM: 1. Connection of the site to a perched aquifer of sufficient size (volume) to buffer rainfall deficits; or 2. Climate along the lower east coast of Australia were not significantly drier than today;

or 3. Despite a reduction in precipitation, lower temperatures reduce the evaporative effect across the wetland.

Welsby Lagoon is predominantly supported by a perched aquifer that extends beyond the surface expression of the wetland (Figure 6). Contemporary observations have shown that the surface water can be lost during annual and inter-annual drought periods; however, during these events the wetland sediments remain inundated by the perched aquifer. Therefore, the buffering effect of the perched aquifer may have contributed to creating a positive moisture balance at this site during dry periods.

NSI would have maintained a relatively coastal position, even during the lowest sea level stands of the LGM, due to its location close to the edge of the continental shelf (Figure 1A). An increasing body of evidence has emerged in the last two decades indicating that regions of Australia were not as arid during the LGM as previously thought (Cohen et al., 2012; Nanson et al., 2008; Petherick et al., 2008; Reeves et al., 2013a; Tibby et al., 2017). The maintenance of a maritime climate during this period may have tempered the effects of a more arid climate seen across other regions of Australia, allowing Welsby Lagoon, and other sites on the island (Moss et al., 2013; Petherick et al., 2017; Tibby et al., 2017), to maintain a positive moisture balance. An increase in water availability may be driven by increased rainfall or reduced evaporation rates resulting from depressed temperatures. The maintenance of organic deposition in the centre of Welsby Lagoon during the LGM indicates a positive moisture was maintained for the entirety of this record. The persistence of a number of wetland sites across NSI during the LGM and presence of arboreal pollen suggest that changes in precipitation were not sufficiently large to cause these wetlands to dry or shift the local vegetation from an open woodland to non-arboreal vegetation system (Moss et al., 2013; Petherick et al., 2017).

5.4 Deglacial and Holocene

The recommencement of peat accumulation after ca. 19 ka on the Welsby Lagoon fringe indicates inundation of the wetland margin and increased moisture balance at the site (Barr et al., 2017). A shift to more moist conditions is also suggested in the centre of the wetland at this time. Terrestrial indicators (swamp herbs and Casuarinaceae anthers) and emergent macrophyte fossils decline after 380 cm (Figure 4). These indicators are closely followed by a decline in sedimentary lignin and an increase in $\delta^{15}N$, implying a reduction in the dominance of aquatic macrophytes (Figure 3). Together these data suggest that our core site at the centre of the wetland reverted to a deeper water system at the beginning of the deglacial.

A permanent palustrine wetland developed during the Holocene (above 260 cm) and is characterised by higher mean lignin, TOC, $\delta^{13}C$ and lower $\delta^{15}N$. It is possible that after the period of increased inputs of organic carbon, driven by the dominance of emergent macrophytes, the wetland crossed a critical threshold of basin infilling. If the level of sediment surface (due to infilling) surpasses the highest level of the perched aquifer (i.e. the perching layer), the water-holding capacity of the site would prevent the development of deep water as any excess would 'overflow' through the sandy regolith. Therefore, the surface expression of the Welsby Lagoon aquifer is dependent on the limit of the perched water table, the morphology of the basin and the depth of sediment surface. The current Welsby Lagoon wetland contains 12.7 m of sediment and is presently a palustrine wetland dominated by emergent sedges (Figure 6). Sediment has largely filled the basin and the present water depth varies seasonally, ranging between 0 and 1.5 m. In conjunction with the palaeolimnological information garnered in this study, it is clear that the Welsby Lagoon basin is approaching the terminal stage of lake succession.

6. Conclusions

We have inferred the evolution of Welsby Lagoon and its interactions with broad scale prevailing climate for the last ca. 130,000 years by considering patterns in the variability of multiple proxies

preserved in the 12.7 m sediment sequence of Welsby Lagoon. The formation of a perching layer in the basin that now supports Welsby Lagoon occurred at ca.130 ka during MIS5e. Continuous sediment deposition began sometime after this and has persisted until present.

The Welsby Lagoon sediments from 1210 cm to 500 cm indicate an open-water lake environment dominated by aquatic algae. Gradual shallowing of the wetland after 825 cm was associated with an increased dominance of emergent aquatic macrophytes and terrestrial swamp herbs. Progressive climatic drying after 800 cm led to a decline in regional rainforest vegetation. After 500 cm the wetland transitioned to a shallower, emergent macrophyte dominated swamp environment.

The interval between 500 and 360 cm was the driest in the history of the site, yet the centre of Welsby Lagoon maintained a positive moisture balance, as indicated by the continued deposition of organic peat. Between 360 – 300 cm there is an indication the site had more areas of open water. Shallow palustrine swamp conditions occur after 300 cm that persist until present.

The understanding garnered from this foundation study provides a strong basis for using this site for further investigations into Australian palaeoclimate and palaeoecology. The development of a robust age model to tightly constrain the record is a key research priority to identify key Quaternary events, such as arrival of humans and extinction of megafauna. The Welsby Lagoon sedimentary record offers an opportunity to become a key Australian sedimentary archive to contribute to an enhanced global understanding of Quaternary climate and ecosystem responses.

Acknowledgments.

We acknowledge Minjerribah (NSI) and the surrounding waters as Quandamooka Country. The study was funded by Australian Research Council project DP150103875. We thank Jie Chang, Jacinta Greer, Matthew Jones, Patrick Moss and Cameron Schulz for assistance in the field. We sincerely thank Fred Oudyn for analysis and data processing of pigment samples with such efficiency and Janine McGowan (CSIRO Agriculture and Food) for assistance with NMR sample analysis and data

processing. We thank Adriana Garcia for assistance with macrofossil identification. Discussions with Carl Sayer, Tim Page and Paul Smith improved our understanding.

Aitken, M.J., 1998. An introduction to optical dating: The dating of Quaternary sediments by the use of photon-stimulated luminescence, Oxford science publications. https://doi.org/10.1002/(SICI)1520-6548(200001)15:1<81::AID-GEA5>3.3.CO;2-Y

Arnold, L.J., Bailey, R.M., Tucker, G.E., 2007. Statistical treatment of fluvial dose distributions from southern Colorado arroyo deposits. Quat. Geochronol. 2, 162–167. https://doi.org/10.1016/j.quageo.2006.05.003

Arnold, L.J., Demuro, M., Navazo, M., Benito-Calvo, A., Pérez-González, A., 2013. OSL dating of the Middle Palaeolithic Hotel California site, Sierra de Atapuerca, north-central Spain. Boreas 42, 285–305. https://doi.org/10.1111/j.1502-3885.2012.00262.x

Arnold, L.J., Duval, M., Demuro, M., Spooner, N.A., Santonja, M., Pérez-González, A., 2016. OSL dating of individual quartz 'supergrains' from the Ancient Middle Palaeolithic site of Cuesta de la Bajada, Spain. Quat. Geochronol. 36, 78–101. https://doi.org/10.1016/j.quageo.2016.07.003

Arnold, L.J., Roberts, R.G., Galbraith, R.F., DeLong, S.B., 2009. A revised burial dose estimation procedure for optical dating of youngand modern-age sediments. Quat. Geochronol. 4, 306–325. https://doi.org/10.1016/j.quageo.2009.02.017

Baldock, J.A., Sanderman, J., Macdonald, L.M., Puccini, A., Hawke, B., Szarvas, S., McGowan, J., 2013. Quantifying the allocation of soil organic carbon to biologically significant fractions. Soil Res. 51, 561. https://doi.org/10.1071/SR12374

Barko, J.W., Gunnison, D., Carpenter, S.R., 1991. Sediment interactions with submersed macrophyte growth and community dynamics. Aquat. Bot. 41, 41–65. https://doi.org/10.1016/0304-3770(91)90038-7

Barr, C., Tibby, J., Marshall, J.C., Mcgregor, G.B., Moss, P.T., Halverson, G.P., Fluin, J., 2013. Combining monitoring, models and palaeolimnology to assess ecosystem response to environmental change at monthly to millennial timescales: The stability of Blue Lake, North Stradbroke Island, Australia. Freshw. Biol. 58, 1614–1630. https://doi.org/10.1111/fwb.12154

Barr, C., Tibby, J., Moss, P.T., Halverson, G.P., Marshall, J.C., McGregor, G.B., Stirling, E., 2017. A 25,000-year record of environmental change from Welsby Lagoon, North Stradbroke Island, in the Australian subtropics. Quat. Int. 449, 106–118. https://doi.org/10.1016/j.quaint.2017.04.011

Birks, H.H., 2002. Plant Macrofossils, in: Smol, J.P., Birks, H.J.B., Last, W.M., Bradley, R.S., Alverson, K. (Eds.), Tracking Environmental Change Using Lake Sediments: Terrestrial, Algal, and Siliceous Indicators. Springer Netherlands, Dordrecht, pp. 49–74. https://doi.org/10.1007/0-306-47668-1_4

Birks, H.H., Birks, H.J.B., 2006. Multi-proxy studies in palaeolimnology. Veg. Hist. Archaeobot. https://doi.org/10.1007/s00334-006-0066-6

Black, M.P., Mooney, S.D., Martin, H.A., 2006. A >43,000-year vegetation and fire history from Lake Baraba, New South Wales, Australia. Quat. Sci. Rev. 25, 3003–3016. https://doi.org/10.1016/j.quascirev.2006.04.006

Blindow, I., 1992. Long- and short-term dynamics of submerged macrophytes in two shallow eutrophic lakes. Freshw. Biol. 28, 15–27. https://doi.org/10.1111/j.1365-2427.1992.tb00558.x

BOM, (Australian Bureau of Meterology), 2018. Climate statistics for Australian locations [WWW Document]. URL http://www.bom.gov.au/climate/averages/tables/cw_040209.shtml (accessed 1.24.18).

Chang, C.C.Y., McCormick, P. V., Newman, S., Elliott, E.M., 2009. Isotopic indicators of environmental change in a subtropical wetland. Ecol. Indic. 9, 825–836.

https://doi.org/10.1016/j.ecolind.2008.09.015

Chang, J.C., Shulmeister, J., Woodward, C., Steinberger, L., Tibby, J., Barr, C., 2015. A chironomid-inferred summer temperature reconstruction from subtropical Australia during the last glacial maximum (LGM) and the last deglaciation. Quat. Sci. Rev. 122, 282–292. https://doi.org/10.1016/j.quascirev.2015.06.006

Chen, C.R., Hou, E.Q., Condron, L.M., Bacon, G., Esfandbod, M., Olley, J., Turner, B.L., 2015. Soil phosphorus fractionation and nutrient dynamics along the Cooloola coastal dune chronosequence, southern Queensland, Australia. Geoderma 257–258, 4–13. https://doi.org/10.1016/j.geoderma.2015.04.027

Chen, X.Y., Barton, C.E., 1991. Onset of aridity and dune-building in central Australia: sedimentological and magnetostratigraphic evidence from Lake Amadeus. Palaeogeogr. Palaeoclimatol. Palaeoecol. 84, 55–73. https://doi.org/10.1016/0031-0182(91)90035-P

Clark, R.L., 1982. Point Count Estimation of Charcoal in Pollen Preparation and Thin Sections of Sediments. Pollen et Spores 24, 523–535.

Clarkson, C., Jacobs, Z., Marwick, B., Fullagar, R., Wallis, L., Smith, M., Roberts, R.G., Hayes, E., Lowe, K., Carah, X., Florin, S.A., McNeil, J., Cox, D., Arnold, L.J., Hua, Q., Huntley, J., Brand, H.E.A., Manne, T., Fairbairn, A., Shulmeister, J., Lyle, L., Salinas, M., Page, M., Connell, K., Park, G., Norman, K., Murphy, T., Pardoe, C., 2017. Human occupation of northern Australia by 65,000 years ago. Nature 547, 306–310. https://doi.org/10.1038/nature22968

Cohen, T.J., Jansen, J.D., 2015. Drying inland seas probably helped kill Australia ' s megafauna.

Cohen, T.J., Nanson, G.C., Jansen, J.D., Jones, B.G., Jacobs, Z., Larsen, J.R., May, J.H., Treble, P., Price, D.M., Smith, A.M., 2012. Late Quaternary mega-lakes fed by the northern and southern river systems of central Australia: Varying moisture sources and increased continental aridity. Palaeogeogr. Palaeoclimatol. Palaeoecol. 356–357, 89–108.

https://doi.org/10.1016/j.palaeo.2011.06.023

D'Costa, D.M., Grindrod, J., Ogden, R., 1993. Preliminary environmental reconstructions from late Quaternary pollen and mollusc assemblages at Egg Lagoon, King Island, Bass Strait. Aust. J. Ecol. 18, 351–366. https://doi.org/10.1111/j.1442-9993.1993.tb00462.x

Drew, S., Flett, I., Wilson, J., Heijnis, H., Skilbeck, C.G., 2008. The trophic history of Myall Lakes, New South Wales, Australia: Interpretations using δ13C and δ15N of the sedimentary record. Hydrobiologia 608, 35–47. https://doi.org/10.1007/s10750-008-9383-3

Finlay, J.C., Kendall, C., 2008. Stable isotope tracing of temporal and spatial variability in organic matter sources to freshwater ecosystems, in: Michener, R., Lajtha, K. (Eds.), Stable Isotopes in Ecology and Environmental Science. Blackwell Publishing Ltd, Oxford, pp. 283–333. https://doi.org/DOI: 10.1002/9780470691854.ch10

Galbraith, R.F., Roberts, R.G., Laslett, G.M., Yoshida, H., Olley, J.M., Galbraith, R.F., Olley, J.M., Yoshida, H., Laslett, G.M., 1999. Optical dating of single and multiple grains of quartz from Jinmium rock shelter, Northern Australia: Part I, Experimetal design and statistical models. Archaeometry 41, 339–364. https://doi.org/10.1111/j.1475-4754.1999.tb00987.x

Gu, B., Schelske, C.L., Brenner, M., 1996. Relationship between sediment and plankton isotope ratios (δ13C and δ15N) and primary productivity in Florida lakes. Can. J. Fish. Aquat. Sci. 53, 875–883. https://doi.org/10.1139/cjfas-53-4-875

Guérin, G., Mercier, N., Adamiec, G., 2011. Dose-rate conversion factors: update. Anc. TL 29, 5–8.

Hamm, G., Mitchell, P., Arnold, L.J., Prideaux, G.J., Questiaux, D., Spooner, N.A., Levchenko, V.A., Foley, E.C., Worthy, T.H., Stephenson, B., Coulthard, V., Coulthard, C., Wilton, S., Johnston, D., 2016. Cultural innovation and megafauna interaction in the early settlement of arid Australia. Nature 539, 280–283. https://doi.org/10.1038/nature20125

Harle, K.J., Heijnis, H., Chisari, R., Kershaw, A.P., Zoppi, U., Jacobsen, G., 2002. A chronology for the

long pollen record from Lake Wangoom, western Victoria (Australia) as derived from uranium/thorium disequilibrium dating. J. Quat. Sci. 17, 707–720. https://doi.org/10.1002/jqs.684

Healey, F.P., Hendzel, L.L., 1980. Physiological Indicators of Nutrient Deficiency in Lake Phytoplankton. Can. J. Fish. Aquat. Sci. 37, 442–453. https://doi.org/10.1139/f80-058

Hecky, R.E., Campbell, P., Hendzel, L.L., 1993. The stoichiometry of carbon, nitrogen, and phosphorus in particulate matter of lakes and oceans. Limnol. Oceanogr. 38, 709–724. https://doi.org/10.4319/lo.1993.38.4.0709

Heyng, A.M., Mayr, C., Lücke, A., Striewski, B., Wastegård, S., Wissel, H., 2012. Environmental changes in northern New Zealand since the Middle Holocene inferred from stable isotope records (δ15N, δ13C) of Lake Pupuke. J. Paleolimnol. 48, 351–366. https://doi.org/10.1007/s10933-012-9606-5

Huang, Y., Street-Perrott, F.A., Perrott, R.A., Metzger, P., Eglinton, G., 1999. Glacial-interglacial environmental changes inferred from molecular and compound-specific δ13C analyses of sediments from Sacred Lake, Mt. Kenya. Geochim. Cosmochim. Acta 63, 1383–1404. https://doi.org/10.1016/S0016-7037(99)00074-5

Johnson, C.N., Rule, S., Haberle, S.G., Kershaw, A.P., McKenzie, G.M., Brook, B.W., 2016. Geographic variation in the ecological effects of extinction of Australia's Pleistocene megafauna. Ecography (Cop.). 39, 109–116. https://doi.org/10.1111/ecog.01612

Juggins, S., 2015. rioja: Anlaysis of Quaternary science data. R Packag. ver. 0.9-5.

Kershaw, A.P., Bretherton, S.C., van der Kaars, S., 2007a. A complete pollen record of the last 230 ka from Lynch's Crater, north-eastern Australia. Palaeogeogr. Palaeoclimatol. Palaeoecol. 251, 23–45. https://doi.org/10.1016/j.palaeo.2007.02.015

Kershaw, A.P., McKenzie, G.M., Porch, N., Roberts, R.G., Brown, J., Heijnis, H., Orr, M.., 2007b. A

high-resolution record of vegetation and climate through the last glacial cycle from Caledonia Fen, southeastern highlands of Australia. J. Quat. Sci. 22, 801–815. https://doi.org/10.1002/jqs

Kershaw, A.P., Nanson, G.C., 1993. The last full glacial cycle in the Australian region. Glob. Planet. Change 7, 1–9. https://doi.org/10.1016/0921-8181(93)90036-N

Laws, E.A., Popp, B.N., Bidigare, R.R., Kennicutt, M.C., Macko, S.A., 1995. Dependence of phytoplankton carbon isotopic composition on growth rate and [CO2)aq: Theoretical considerations and experimental results. Geochim. Cosmochim. Acta 59, 1131–1138. https://doi.org/10.1016/0016-7037(95)00030-4

Leach, L.M., 2011. Hydrological and physical setting of North Stradbroke Island. Proc. R. Soc. Queensl. 117, 21–46.

Leavitt, P.R., Hodgson, D.A., 2002. Sedimentary Pigments, in: Tracking Environmental Change Using Lake Sediments. pp. 295–325. https://doi.org/10.1007/0-306-47668-1_15

Lee, R.E., 2008. Phycology, 4th ed. Cambridge University Press, New York.

Lees, B., 2006. Timing and Formation of Coastal Dunes in Northern and Eastern Australia. J. Coast. Res. 221, 78–89. https://doi.org/10.2112/05A-0007.1

Leng, M.J., 2006. Isotopes in Paleoenvironmental Research.

Leng, M.J., Marshall, J.D., 2004. Palaeoclimate interpretation of stable isotope data from lake sediment archives. Quat. Sci. Rev. 23, 811–831. https://doi.org/10.1016/j.quascirev.2003.06.012

Lewis, T., 2012. A plant macrofossil identification tool for south-west Victoria. The Artefact 35, 88–98.

Longmore, M.E., 1997. Quaternary Palynological Records from Perched Lake Sediments, Fraser Island, Queensland, Australia: Rainforest, Forest History and Climatic Control. Aust. J. Bot. 45,

507–526. https://doi.org/10.1071/BT96109

Marshall, J.C., McGregor, G.B., 2011. The influence of water depth on the distribution of the emergent sedge Lepironia articulata (Cyperaceae) in two dune lakes of southern Queensland Coastal Wallum Wetlands. Proc. R. Soc. Queensl. 117, 193–199.

Mayr, C., Lücke, A., Maidana, N.I., Wille, M., Haberzettl, T., Corbella, H., Ohlendorf, C., Schäbitz, F., Fey, M., Janssen, S., Zolitschka, B., 2009. Isotopic fingerprints on lacustrine organic matter from Laguna Potrok Aike (southern Patagonia, Argentina) reflect environmental changes during the last 16,000 years. J. Paleolimnol. 42, 81–102. https://doi.org/10.1007/s10933-008-9249-8

Mejdahl, V., 1979. Thermoluminescence Dating: Beta-Dose Attenuation in Quartz Grains. Archaeometry 21, 61–72. https://doi.org/10.1111/j.1475-4754.1979.tb00241.x

Mettam, P., Tibby, J., Barr, C., Marshall, J.C., 2011. Development of Eighteen Mile Swamp, North Stradbroke Island: a palaeolimnological study. Proc. R. Soc. Queensl. 117, 119–131.

Meyers, P.A., Arbor, A., 2001. Sediment organic Matter 2, 239–269.

Meyers, P.A., Teranes, J.L., 2001. Sediment organic Matter, in: Last, W.M., Smol, J.P. (Eds.), Tracking Environmental Change Using Lake Sediments. Volume 2. pp. 239–269.

Miot da Silva, G., Shulmeister, J., 2016. A Review of Coastal Dunefield Evolution in Southeastern Queensland. J. Coast. Res. 75, 308–312. https://doi.org/10.2112/SI75-062.1

Moss, P.T., Kershaw, A.P., 2000. The last glacial cycle from the humid tropics of northeastern Australia: Comparison of a terrestrial and a marine record. Palaeogeogr. Palaeoclimatol. Palaeoecol. 155, 155–176. https://doi.org/10.1016/S0031-0182(99)00099-1

Moss, P.T., Petherick, L., Neil, D., 2011. Environmental Change at Myora Springs, North Stradbroke Island Over the Last Millenium. Proc. R. Soc. Queensl. 117, 113–140.

Moss, P.T., Tibby, J., Petherick, L., McGowan, H., Barr, C., 2013. Late Quaternary vegetation history

of North Stradbroke Island, Queensland, eastern Australia. Quat. Sci. Rev. 74, 257–272. https://doi.org/10.1016/j.quascirev.2013.02.019

Murray, A.S., Wintle, A.G., 2000. Luminescence dating of quartz using an improved single-aliquot regenerative-dose protocol. Radiat. Meas. 32, 57–73. https://doi.org/10.1016/S1350-4487(99)00253-X

Myrbo, A., Wright, H.E., 2008. SOP: Livingstone-bolivia.

Nanson, G.C., Price, D.M., Jones, B.G., Maroulis, J.C., Coleman, M., Bowman, H., Cohen, T.J., Pietsch, T.J., Larsen, J.R., 2008. Alluvial evidence for major climate and flow regime changes during the middle and late Quaternary in eastern central Australia. Geomorphology 101, 109–129. https://doi.org/10.1016/j.geomorph.2008.05.032

Petherick, L., McGowan, H., Moss, P., 2008. Climate variability during the Last Glacial Maximum in eastern Australia: Evidence of two stadials? J. Quat. Sci. 23, 787–802. https://doi.org/10.1002/jqs.1186

Petherick, L.M., Moss, P.T., McGowan, H.A., 2017. An extended Last Glacial Maximum in subtropical Australia. Quat. Int. 432, 1–12. https://doi.org/10.1016/j.quaint.2015.11.015

Petherick, L.M., Moss, P.T., McGowan, H.A., 2011. Climatic and environmental variability during the termination of the Last Glacial Stage in coastal eastern Australia: A review. Aust. J. Earth Sci. 58, 563–577. https://doi.org/10.1080/08120099.2011.566281

Prescott, J.R., Hutton, J.T., 1994. Cosmic ray contributions to dose rates for luminescence and ESR dating: Large depths and long-term time variations. Radiat. Meas. 23, 497–500. https://doi.org/10.1016/1350-4487(94)90086-8

Pye, K., 1993. Late Quaternary development of coastal parabolic megadune complexes in northeastern Australia, in: Pye, K., Lancaster, N. (Eds.), Aeolian Sediments : Ancient and Modern. Blackwell Scientific Publications, p. 167.

R Core Team, 2017. R: A Language and Environment for Statistical Computing. R Found. Stat. Comput. Vienna, Austria. https://doi.org/http://www.R-project.org/

Reeves, J.M., Barrows, T.T., Cohen, T.J., Kiem, A.S., Bostock, H.C., Fitzsimmons, K.E., Jansen, J.D., Kemp, J., Krause, C., Petherick, L., Phipps, S.J., Armand, L.K., Ayliffe, L.K., Curran, M., De Deckker, P., Devriendt, L.S., Dodson, J., Dosseto, A., Dunbar, G.B., Drysdale, R.N., Fink, D., Fischer, M., Fletcher, M.S., Fujioka, T., Gagan, M.K., Griffiths, M.L., Haberlah, D., Haberle, S.G., Heikkila, U., Heijnis, H., Hesse, P.P., Hilgers, A., Ho, M., Howard, W., Hua, Q., Kelly, T., Larsen, J., Lewis, S., Lomax, J., Mackintosh, A., May, J.H., McGregor, H. V., Meisner, K., Mooney, S.D., Moss, P.T., Nanson, G.C., Pedro, J., Purcell, A., Shulmeister, J., Sloss, C., Swander, Z., Tibby, J., Treble, P., Van Der Kaars, S., White, D., Woodward, C., 2013a. Climate variability over the last 35,000 years recorded in marine and terrestrial archives in the Australian region: An OZ-INTIMATE compilation. Quat. Sci. Rev. 74, 21–34. https://doi.org/10.1016/j.quascirev.2013.01.001

Reeves, J.M., Bostock, H.C., Ayliffe, L.K., Barrows, T.T., De Deckker, P., Devriendt, L.S., Dunbar, G.B., Drysdale, R.N., Fitzsimmons, K.E., Gagan, M.K., Griffiths, M.L., Haberle, S.G., Jansen, J.D., Krause, C., Lewis, S., McGregor, H. V., Mooney, S.D., Moss, P., Nanson, G.C., Purcell, A., van der Kaars, S., 2013b. Palaeoenvironmental change in tropical Australasia over the last 30,000 years - a synthesis by the OZ-INTIMATE group. Quat. Sci. Rev. 74, 97–114. https://doi.org/10.1016/j.quascirev.2012.11.027

Roberts, R.G., Flannery, T.F., Ayliffe, L.K., Yoshida, H., Olley, J.M., Prideaux, G.J., Laslett, G.M., Baynes, A., Smith, M.A., Jones, R., Smith, B.L., 2001. New ages for the last Australian megafauna: continent-wide extinction about 46,000 years ago. Science 292, 1888–92. https://doi.org/10.1126/science.1060264

Roy, S., Llewellyn, C., Egeland, E.S., Johnsen, G., 2011. Phytoplankton Pigments: Characterization, Chemotaxonomy and Applications in Oceanography., Cambridge environmental chemistry

series. Cambridge University Press, Cambridge. https://doi.org/10.1111/jpy.12035

Rule, S., Brook, B.W., Haberle, S.G., Turney, C.S.M., Kershaw, A.P., Johnson, C.N., 2012. The Aftermath of Megafaunal Extinction: Ecosystem Transformation in Pleistocene Australia. Science (80-.). 335, 1483–1486. https://doi.org/10.1126/science.1214261

Sanger, J.E., 1988. Fossil pigments in paleoecology and paleolimnology. Palaeogeogr. Palaeoclimatol. Palaeoecol. 62, 343–359. https://doi.org/10.1016/0031-0182(88)90061-2

Saunders, M.J., Kansiime, F., Jones, M.B., 2014. Reviewing the carbon cycle dynamics and carbon sequestration potential of Cyperus papyrus L. wetlands in tropical Africa. Wetl. Ecol. Manag. 22, 143–155. https://doi.org/10.1007/s11273-013-9314-6

Schlesinger, W.H., Bernhardt, E.S., 2013. Biogeochemistry: An Analysis of Global Change, 3rd Editio. ed, Third Edition. Academic Press. https://doi.org/http://dx.doi.org/10.1016/B978-0-08-091680-4.00001-9

Singh, G., Opdyke, N.D., Bowler, J.M., 1981. Late Cainozoic stratigraphy, palaeomagnetic chronology and vegetational history from Lake George, N.S.W. J. Geol. Soc. Aust. 28, 435–452. https://doi.org/10.1080/00167618108729180

Specht, A., Stubbs, B.J., 2011. Long-term monitoring of a coastal sandy freshwater wetland: Eighteen Mile Swamp, North Stradbroke Island, Queensland. Proc. R. Soc. Queensl. December, 201–223.

Stephens, K.M., Sharp, D., 2009. The flora of North Stradbroke Island. State of Queensland, Environmental Protection Agency.

Talbot, M.R., 2001. Nitrogen Isotopes in Palaeolimnology, in: Tracking Environmental Change Using Lake Sediments. pp. 401–439.

Talbot, M.R., Lærdal, T., 2000. The Late Pleistocene - Holocene palaeolimnology of Lake Victoria, East Africa, based upon elemental and isotopic analyses of sedimentary organic matter. J.

Paleolimnol. 23, 141–164. https://doi.org/10.1023/A:1008029400463

Thompson, C.H., 1981. Podzol chronosequences on coastal dunes of eastern Australia. Nature. https://doi.org/10.1038/291059a0

Tibby, J., Barr, C., Marshall, J.C., McGregor, G.B., Moss, P.T., Arnold, L.J., Page, T.J., Questiaux, D., Olley, J., Kemp, J., Spooner, N., Petherick, L., Penny, D., Mooney, S., Moss, E., 2017. Persistence of wetlands on North Stradbroke Island (south-east Queensland, Australia) during the last glacial cycle: implications for Quaternary science and biogeography. J. Quat. Sci. 32, 770–781. https://doi.org/10.1002/jqs.2981

Timms, B., 1986. The coastal dune lakes of eastern Australia, in: Deckker, P., Williams, W.D. (Eds.), Limnology in Australia. Springer Netherlands, p. 688.

Turney, C.S.M., Haberle, S.G., Fink, D., Kershaw, A.P., Barbetti, M., Barrows, T.T., Black, M., Cohen, T.J., Correge, N.J., Zhao, J. xin, D'Costa, D.M., Feng, Y. xing, Gagan, M.K., Mooney, S.D., Xia, Q., 2006. Integration of ice-core, marine and terrestrial records for the Australian Last Glacial Maximum and Termination: a contribution from the OZ INTIMATE group. J. Quat. Sci. 21, 751–761.

Turney, C.S.M., Kershaw, a P., Clemens, S.C., Branch, N., Moss, P.T., Fifield, L.K., 2004. Millennial and orbital variations of El Niño/Southern Oscillation and high-latitude climate in the last glacial period. Nature 428, 306–10. https://doi.org/10.1038/nature02386

Van Der Kaars, S., De Deckker, P., 2002. A late quaternary pollen record from deep-sea core Fr10/95, GC17 offshore Cape Range Peninsula, northwestern Western Australia. Rev. Palaeobot. Palynol. 120, 17–39. https://doi.org/10.1016/S0034-6667(02)00075-1

Vitousek, P.M., Cassman, K., Cleveland, C., Crews, T., Field, C.B., Grimm, N.B., Howarth, R.W., Marino, R., Martinelli, L., Rastetter, E.B., Sprent, J.I., 2002. Towards an ecological understanding of biological nitrogen fixation. Biogeochemistry.

https://doi.org/10.1023/A:1015798428743

Walker, J., Thompson, C.H., Fergus, I.F., Tunstall, B.R., 1981. Plant Succession and Soil Development in Coastal Sand Dunes of Subtropical Eastern Australia, in: West, D.C., Shugart, H.H., Botkin, D.B. (Eds.), Forest Succession. Springer Advanced Texts in Life Sciences. Springer., New York, NY, pp. 107–131. https://doi.org/10.1007/978-1-4612-5950-3_9

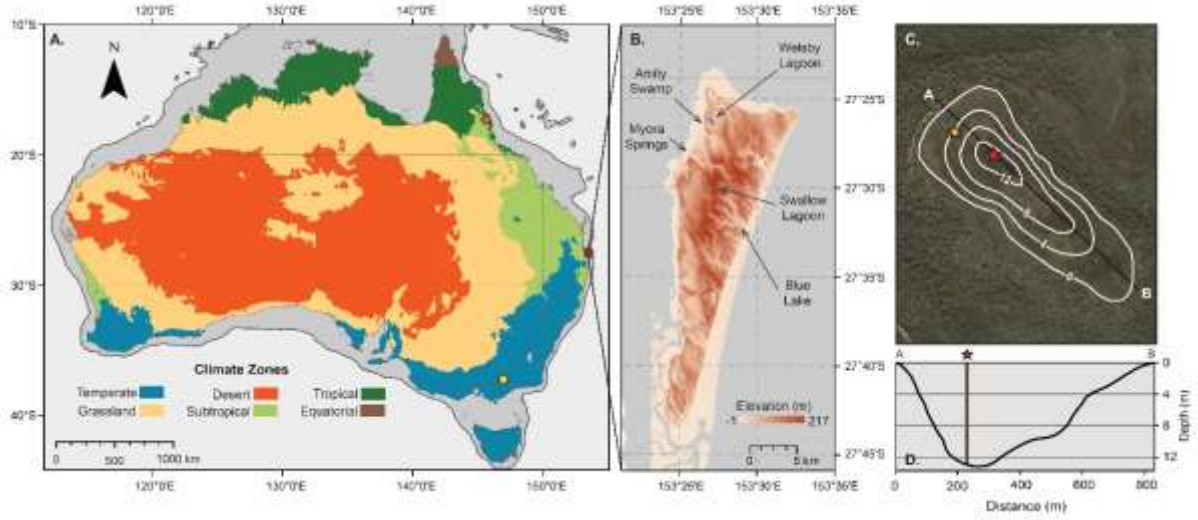

Figure 1. **A.** Map of Australia showing the major Köppen climate zones (BOM, 2018b) and maximum extent of exposed continental shelf (dark grey) during the last glacial maximum. Orange circle indicates location of Lynch's Crater, yellow circle indicates location of Caledonia Fen. **B.** Location of North Stradbroke Island, Welsby Lagoon and other sites named in the text. Shading shows sand dune elevation on the Island (Gallant et al., 2011). **C.** Satellite image of Welsby Lagoon (source: Google Earth). Contours denote basin sediment depth (m) determined from a series of probing transects and interpolated in ArcMap 10.3.1 using the IDW kriging tool. Red star denotes coring location of this study, orange star denotes coring location from Barr et al., 2017. **D.** Depth profile of the Welsby Lagoon basin between points A and B in panel C.

Table 1. Dose rate data, equivalent doses (D_e), overdispersion values, and OSL ages for lacustrine samples from Welsby Lagoon, North Stradbroke Island. The final OSL age of each sample has been calculated by dividing the D_e value by the total dose rate.

Sample (core)	Depth (cm)	Grain size (μm)	Water Content (% Dry) [a]	Environmental dose rate (Gy/ka) [b,c,d,e,f]					Equivalent dose (D_e) data				D_e (Gy) [f]	Final age (ka) [f,k]
				Beta dose rate	Gamma dose rate	Internal dose rate	Cosmic dose rate	Total dose rate	D_e type [g]	No. of grains [h]	Overdispersion (σ_b) (%) [i]	Age Model [g]		
WL15-2(3) (2015)	380	180-250	505/629/923	0.01±0.001	0.01±0.001	0.02±0.007	0.02±0.002	0.05±0.008	SG OSL	82	117	MAM-4_{UL}	0.94±0.15	18.6±4.1
WL15-2(6) (2015)	510	180-250	575/620/945	0.04±0.01	0.05±0.001	0.02±0.007	0.01±0.002	0.12±0.01	SG OSL	113	34	CAM	5.46±0.22	43.7±5.4
GU5.1 (2011)	1268	180-212	247/247/761	0.06±0.009	0.08±0.005	0.03±0.01	0.01±0.001	0.19±0.02	SG OSL	64	15	CAM	24.5±0.6	130±15.3

[a] Long-term water contents used for beta / gamma / cosmic-ray dose rate attenuation, expressed as % of dry mass of mineral fraction, with an assigned relative uncertainty of ±5% (WL15 samples) or ±10% (GU5.1). The final beta dose rates have been adjusted for moisture attenuation using the measured water contents determined from the midpoint of each OSL sample depth. The final gamma dose rates have been adjusted using the average water content measured from each OSL sample midpoint, as well as from 1 cm^3 bulk sediment samples collected 10 cm above and 10 cm below the OSL sample midpoint. The final cosmic-ray dose rates have been adjusted using the average water content measured from 1 cm^3 bulk sediment samples collected at 10 cm intervals throughout the overlying core sequence.

[b] Beta, gamma and internal dose rates have been calculated on dried and powdered sediment samples using ICP-MS and ICP-OES (WL15 samples) or high-resolution gamma spectrometry (GU5.1).

[c] Radionuclide concentrations have been converted to alpha, beta and gamma dose rates using the published conversion factors of , allowing for beta-dose attenuation (Mejdahl, 1979; Brennan, 2003) and long-term water content correction (Aitken, 1985).

[d] An internal dose rate of 0.02 ± 0.01 Gy / ka has been included in the final dose rate calculations of samples WL15-2(3) and WL15-2(6), based on ICP-MS U and Th measurements made on etched quartz grains from associated aeolian deposits at Welsby Lagoon (Lewis et al., in prep) and an alpha efficiency factor (*a* value) of 0.04 ± 0.01 (Rees-Jones, 1995; Rees-Jones & Tite, 1997). Tibby et al. (2017) assigned an assumed internal dose rate of 0.03 ± 0.01 Gy / ka to sample GU5.1, following Bowler et al. (2003).

[e] Cosmic-ray dose rates were calculated using the approach of Prescott & Hutton (1994), and assigned a relative uncertainty of ±10%.

[f] Mean ± total uncertainty (68% confidence interval), calculated as the quadratic sum of the random and systematic uncertainties.

[g] SG OSL = single-grain optically stimulated luminescence; MAM-4_{UL} = Unlogged four-parameter minimum age model (Arnold et al., 2009) ; CAM = Central age model (Galbraith et al., 1999).

[h] Number of D_e measurements that passed the SAR quality assurance criteria and were used for D_e determination.

[i] The relative spread in the D_e dataset beyond that associated with the measurement uncertainties for individual D_e values, calculated using the CAM (WL15-2(6)) or CAM_{UL} (WL15-2(3)).

[j] Total uncertainty includes a systematic component of ±2% associated with laboratory beta-source calibration.

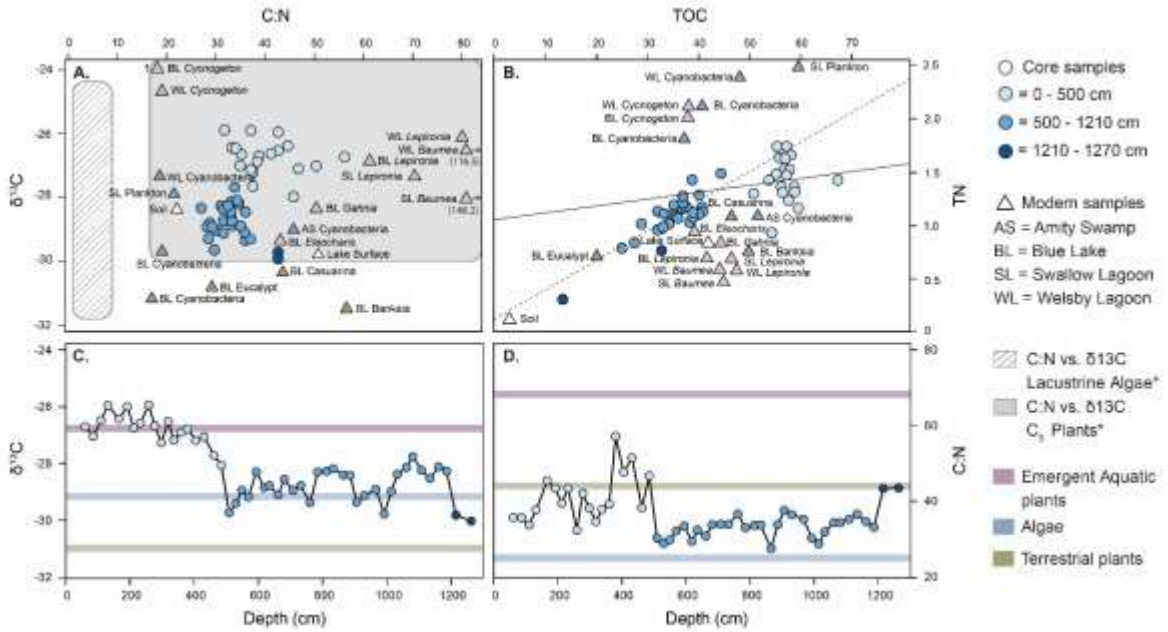

Figure 2. **A.** Carbon isotopes vs. carbon:nitrogen (C:N) ratio of core samples (circles) and modern samples (triangles). **B.** Total organic carbon (TOC) vs. Total nitrogen (TN) of core samples (circles) and modern samples (triangles). Regression line for samples from 0 – 500 cm is show as a solid line and regression line for samples from 500 – 1210 cm is shown as a dashed line. Assuming a linear relationship between TOC and TN, the amount on inorganic nitrogen (IN) is defined as the y-axis intercept (0 – 500 cm IN = 1.0%; 500 – 1210 cm IN = 0.05%) **C**. Sediment $\delta^{13}C$ plotted by depth with averages of modern sample shown in A and B. **D.** Sediment C:N plotted by depth with modern sample averages. Colours of modern samples in all panels correspond to designation as emergent aquatic plants, lacustrine algae and terrestrial plants. *adapted from Meyers and Terranes 2001.

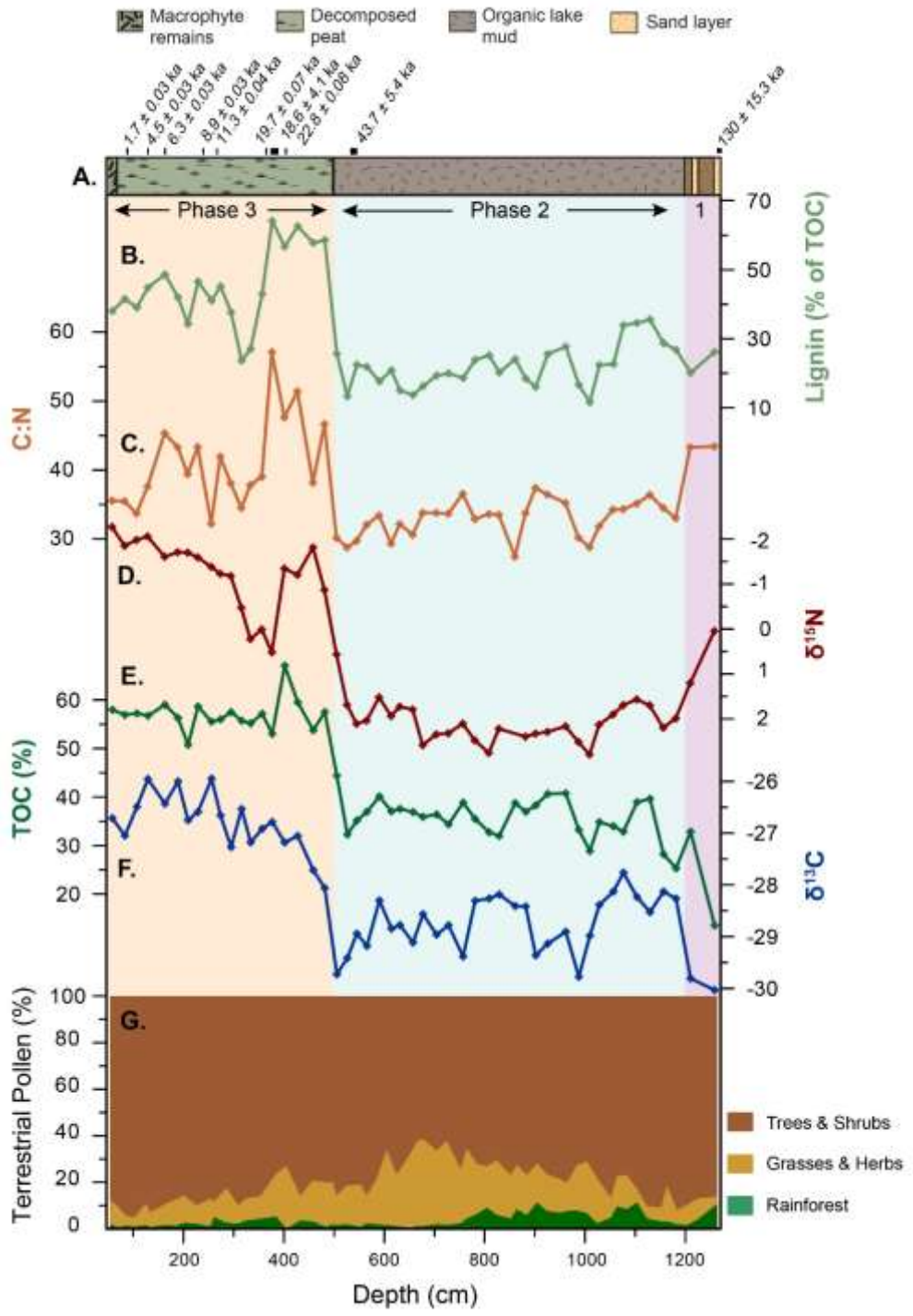

Figure 3. Summary plot of Welsby Lagoon data **A.** stratigraphic profile of 12.7 m Welsby Lagoon sedimentary sequence with description of the lithological units indicated above. Location of radiocarbon (^{14}C) and optically stimulated luminescence (OSL) dates from this study and basal date from Tibby et al. (2017) shown above the stratigraphic profile. **B**. Proportion of TOC identified as lignin from ^{13}C NMR. **C**. C:N ratio. **D**. δ^{15}N (note inverted scale). **E**. TOC %. **F.** δ^{13}C. **G**. Summed terrestrial pollen of sclerophyllous trees and shrubs, grass and herb pollen and rainforest pollen percentages. Shading denotes the three broad phases identified in the wetland record; purple = Phase 1, blue = Phase 2, orange = Phase 3.

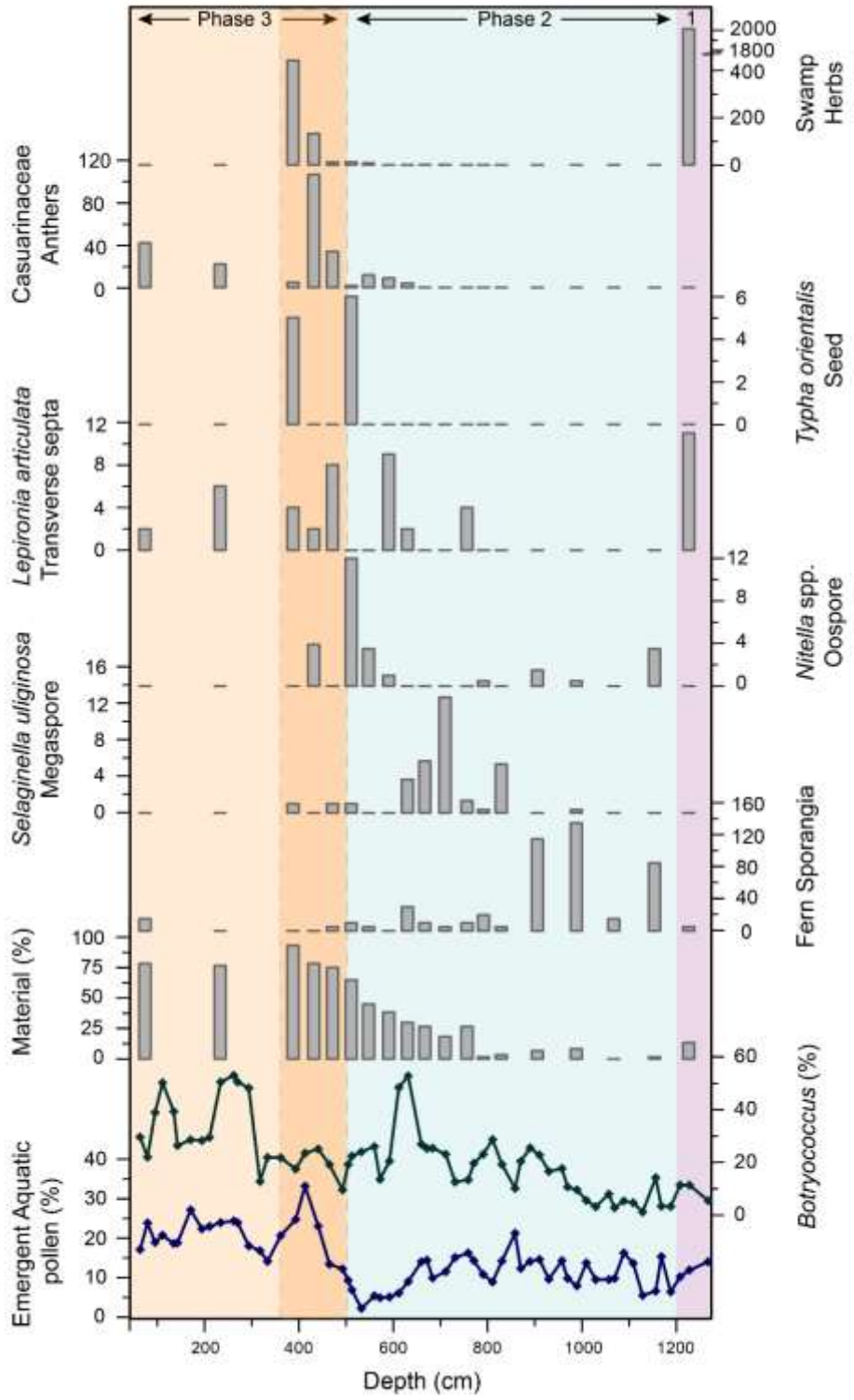

Figure 4. Macrofossil and aquatic pollen summary plot. Macrofossil count data includes all material >125 µm. Emergent aquatic pollen percentage is based on a super sum of all terrestrial and aquatic pollen taxa. *Botryococcus* percentage is based on a super sum of all terrestrial, aquatic and algal taxa. Macrofossil % material is calculated from a 5 mL aliquot of the >250 µm macrofossil sample. Swamp herbs include *Goodenia paniculata (*seed), Cyperaceae (nut), *Gonocarpus* cf. *micranthus* sub

sp. *ramosissimus* (seed), cf. *Drosera* (seed), *Utricularia* (seed), *Cyperus polystachyos var. polystachyos* (nut), *Lobelia anceps* (seed) and *Hydrocotyle verticillata* (mericarp). Shading denotes the three broad phases identified in the wetland record; purple = Phase 1, blue = Phase 2, orange = Phase 3.

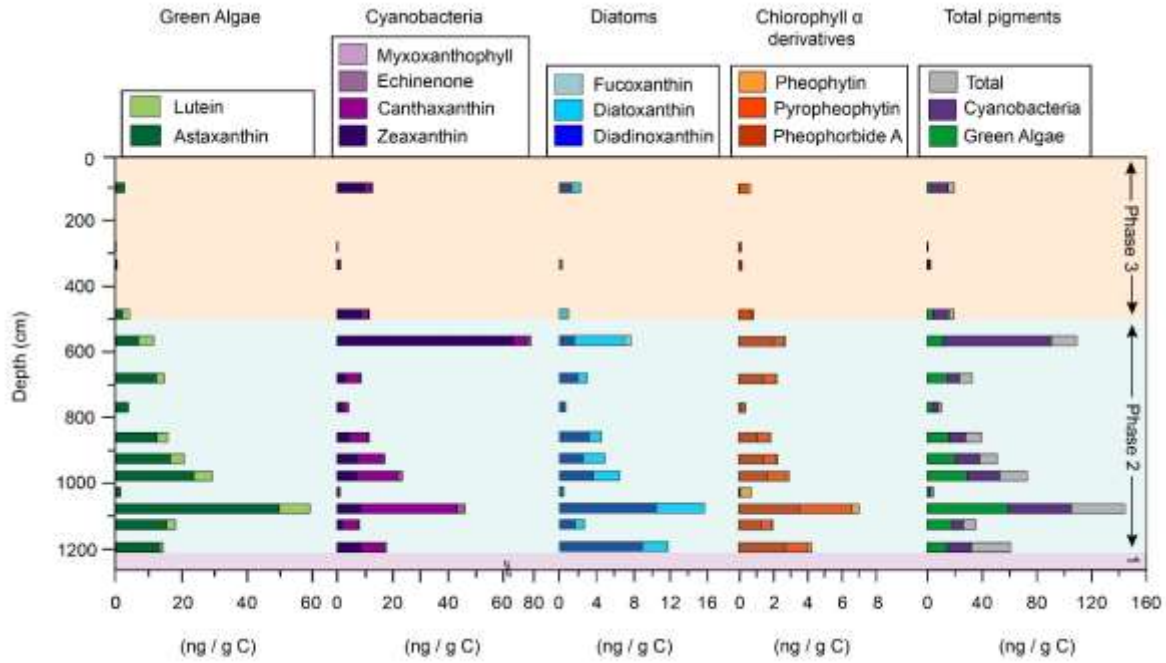

Figure 5. Sedimentary pigment concentration data grouped according to most likely major sources determined from Leavitt and Hodgson (2002) and Roy et al. (2011). All pigment concentrations are expressed as a portion of TOC. Shading denotes the three broad phases identified in the wetland record; purple = Phase 1, blue = Phase 2, orange = Phase 3. Leavitt and Hodgson (2002) and Roy et al. (2011).

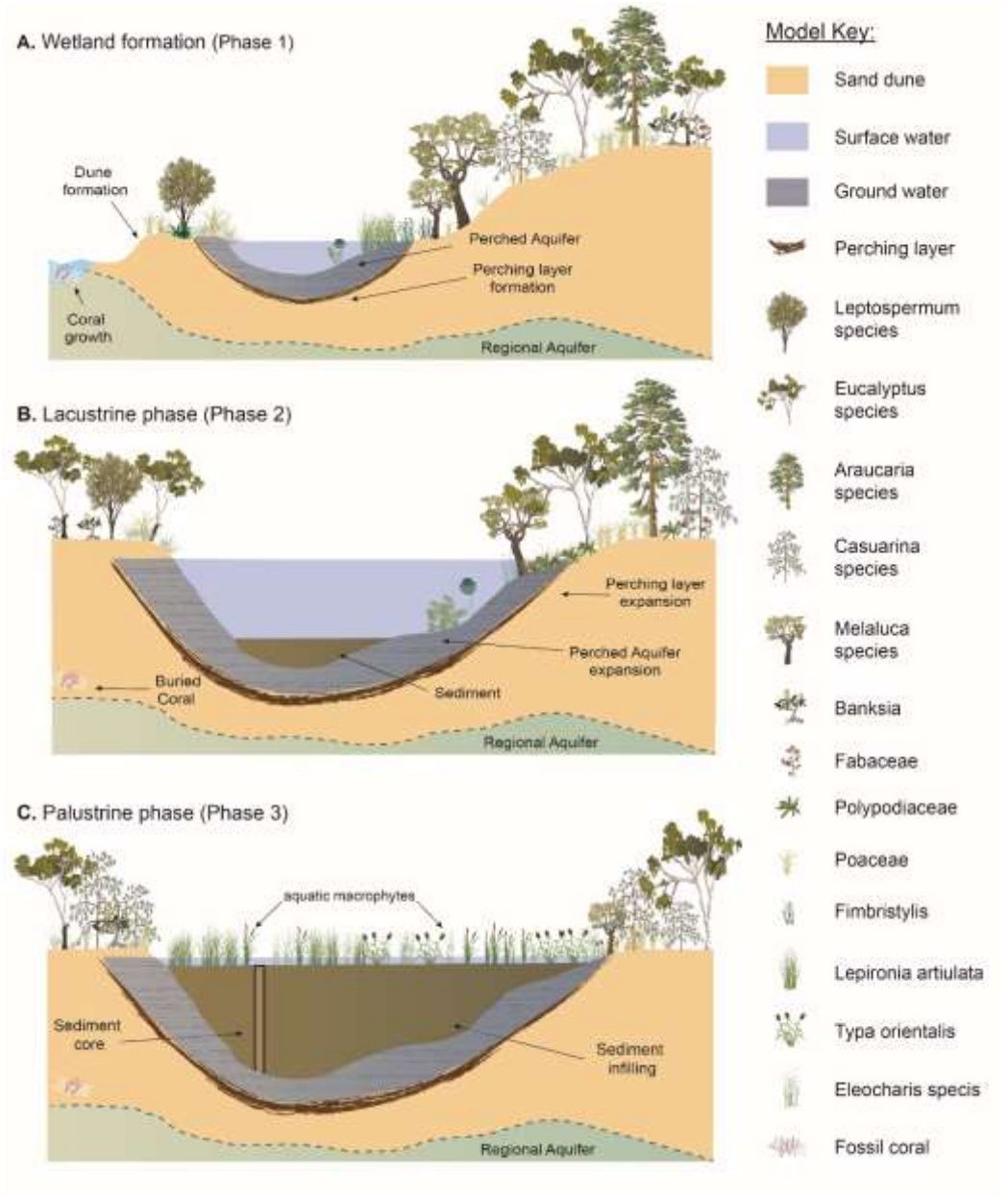

Figure 6. Welsby Lagoon development conceptual model of the **A.** development of the wetland, **B.** evolution through an algal dominated lacustrine system, and **C.** macrophyte dominated shallow swamp phase. Basin morphology defined from basin profile determined in Figure 1. Vegetation images from Integration and Application Network (2018).

Supplementary Information:

Single-grain OSL dating

A total of 500 individual quartz grains from each sample were analysed for equivalent dose (D_e) determination using the single-aliquot regenerative-dose (SAR) method outlined in Table S1. In total, 16 % of measured grains from sample WL15-2(3) and 23 % of measured grains from sample WL15-2(6) were considered suitable for single grain OSL dating after applying the quality assurance criteria outlined in Table S2.

The D_e dataset of sample WL15-2(6) exhibits moderate overdispersion of 34% (Table S3, Figure S1b), which is consistent at 2σ with the overdispersion values obtained for well-bleached and unmixed aeolian deposits at Welsby Lagoon (Lewis et al., in prep). The final burial dose of this sample has therefore been calculated using the central age model (CAM) (Galbraith et al., 1999). The D_e dataset of sample WL15-2(3) is characterised by enhanced inter-grain scatter and a much higher overdispersion value of 117% (Table S3, Figure S1a). These D_e distribution characteristics are interpreted as reflecting insufficient bleaching of some grains prior to deposition and burial (e.g., (Olley et al., 2004, Bailey and Arnold, 2006). This sample also contains a significant number of grains with near-zero Gy D_e values; 34% of accepted grains having individual D_e values consistent with 0 Gy at 2σ. The final burial dose of this sample has therefore been calculated using the four-parameter unlogged minimum age model of Arnold et al. (2009).

Table S1: Single-aliquot regenerative-dose (SAR) procedures used for D_e determination. L_x = regenerative-dose OSL signal response; L_n = natural dose OSL signal response; T_x = test dose OSL signal response for a laboratory dose cycle T_n = test dose OSL signal response for the natural dose cycle.

OSL SAR procedure		
Step	Treatment	Signal
1	Give dose (natural or laboratory)	
2[a]	IRSL stimulation (50°C for 60 s)	
3	Preheat 1 (PH_1 = 260°C for 10 s)	
4	Single grain OSL stimulation (125°C for 2 s)	L_n or L_x
5	Test dose (9-10 Gy)	
6	Preheat 2 (PH_2 = 160°C for 10 s)	
7	Single grain OSL stimulation (125°C for 2 s)	T_n or T_x
8	Repeat cycle for different regenerative doses	

[a] Step 2 is only included in the single-grain OSL SAR procedure when measuring the OSL IR depletion ratio (Duller, 2003).

Table S2: Single grain OSL classification statistics for the Welsby Lagoon sequence samples, following the quality assurance criteria of Arnold et al. (2007). The proportion of grains that were rejected from the final D_e estimation after applying the various quality assurance criteria are shown in rows 7-13.

Sample name	WL15-2(3)	WL15-2(6)
Depth (cm)	380	510
SAR protocol	SG OSL	SG OSL
Total measured grains	500	500
Reason for rejecting grains from De analysis		
Standard SAR rejection criteria:	%	%
Tn <3σ background	60.6	44.6
Dose recycling ratio ≠ 1 at ±2σ	8	14.6
OSL-IR depletion ratios <1 at ±2σ	3	4.8
0 Gy L_x/T_x >5% L_n/T_n	0.8	0.0
Additional rejection criteria:		
Saturated grains (Ln/Tn ≥ dose response curve Imax at ±2σ)	0.4	0.0
Anomalous dose response / unable to perform Monte Carlo fit	10.8	13.2
Sum of rejected grains (%)	83.6	77.2
Sum of accepted grains (%)	16.4	22.8

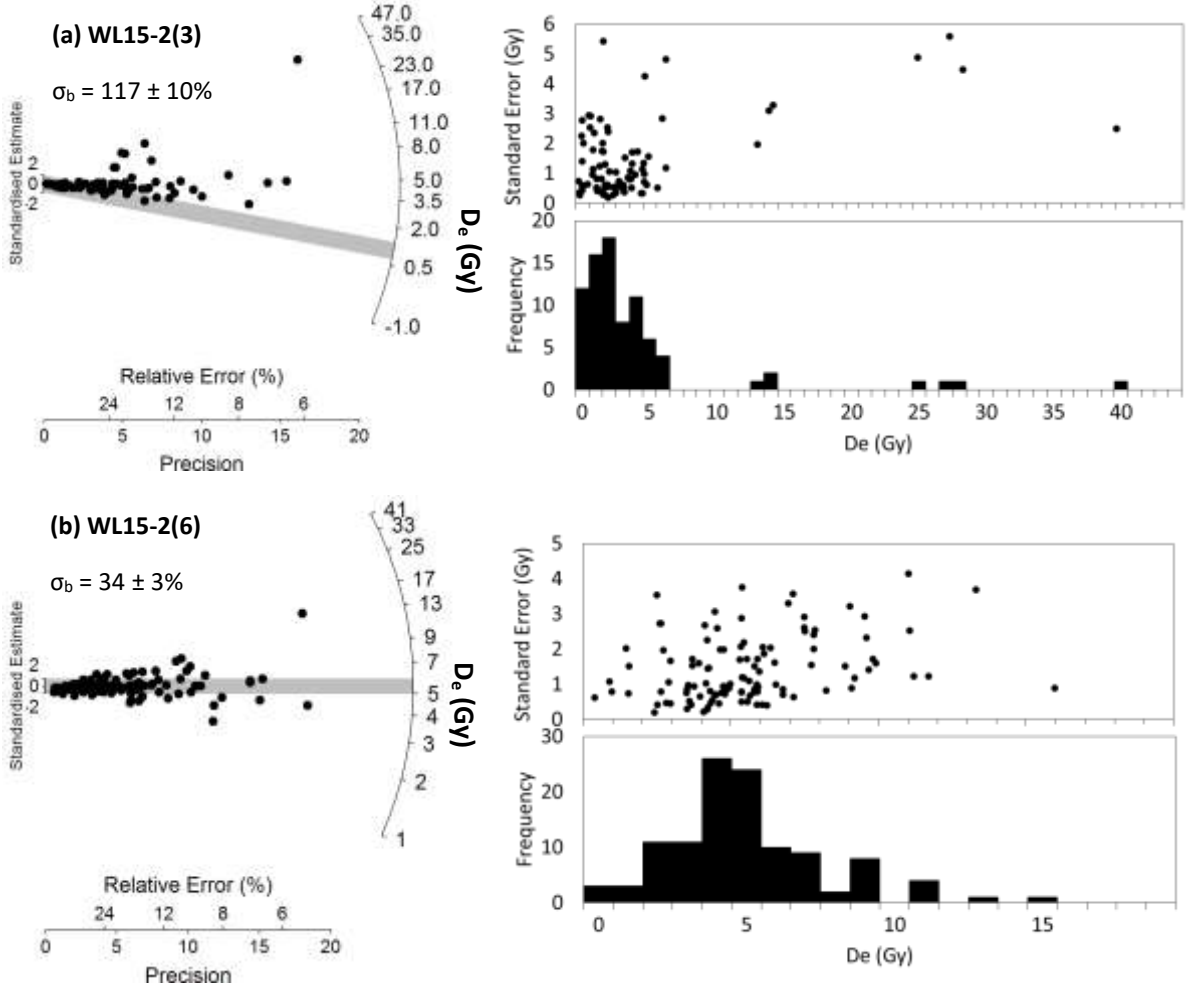

Figure S1: Single-grain D_e distributions for samples (a) WL15-2(3) and (b) WL15-2(6) shown as radial plots and frequency histograms with ranked plots of D_e versus standard error. The grey bars on the radial plots are centred on the D_e values used to derive the final burial dose estimate for each sample (i.e., MAM-4$_{UL}$ for WL2(3) and CAM for WL2(6); (Galbraith et al., 1999, Arnold et al., 2009).

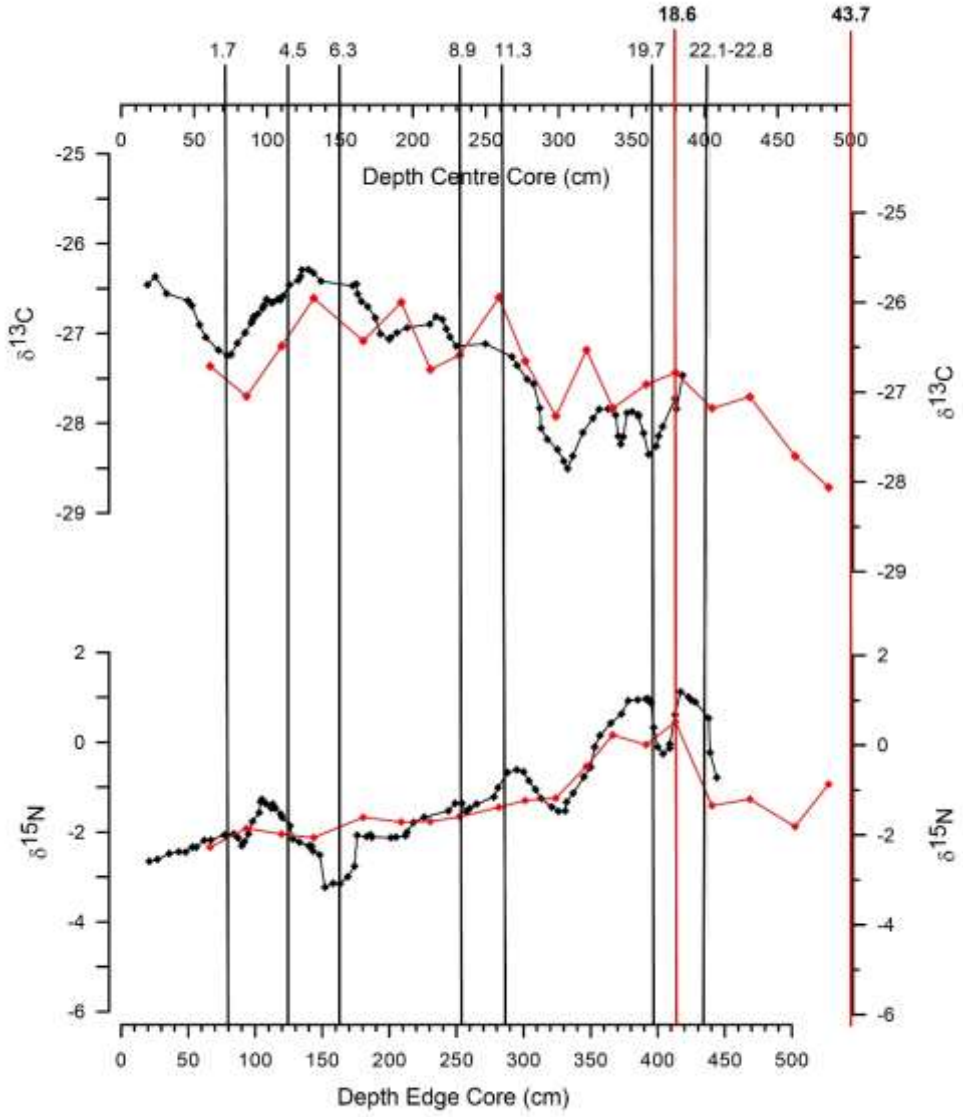

Figure S2. Sediment $\delta^{13}C$ and $\delta^{15}N$ from this study (red) compared with sediment $\delta^{13}C$ and $\delta^{15}N$ from a core taken from the edge of the Welsby Lagoon wetland (black; Barr et al., 2017). Radiocarbon ages from the wetland edge core were recalibrated from Moss et al. (2013) and are shown with vertical black lines with calibrated ages (ka) shown above. Red lines indicate the OSL samples from this study with ages (ka) shown in bold above.

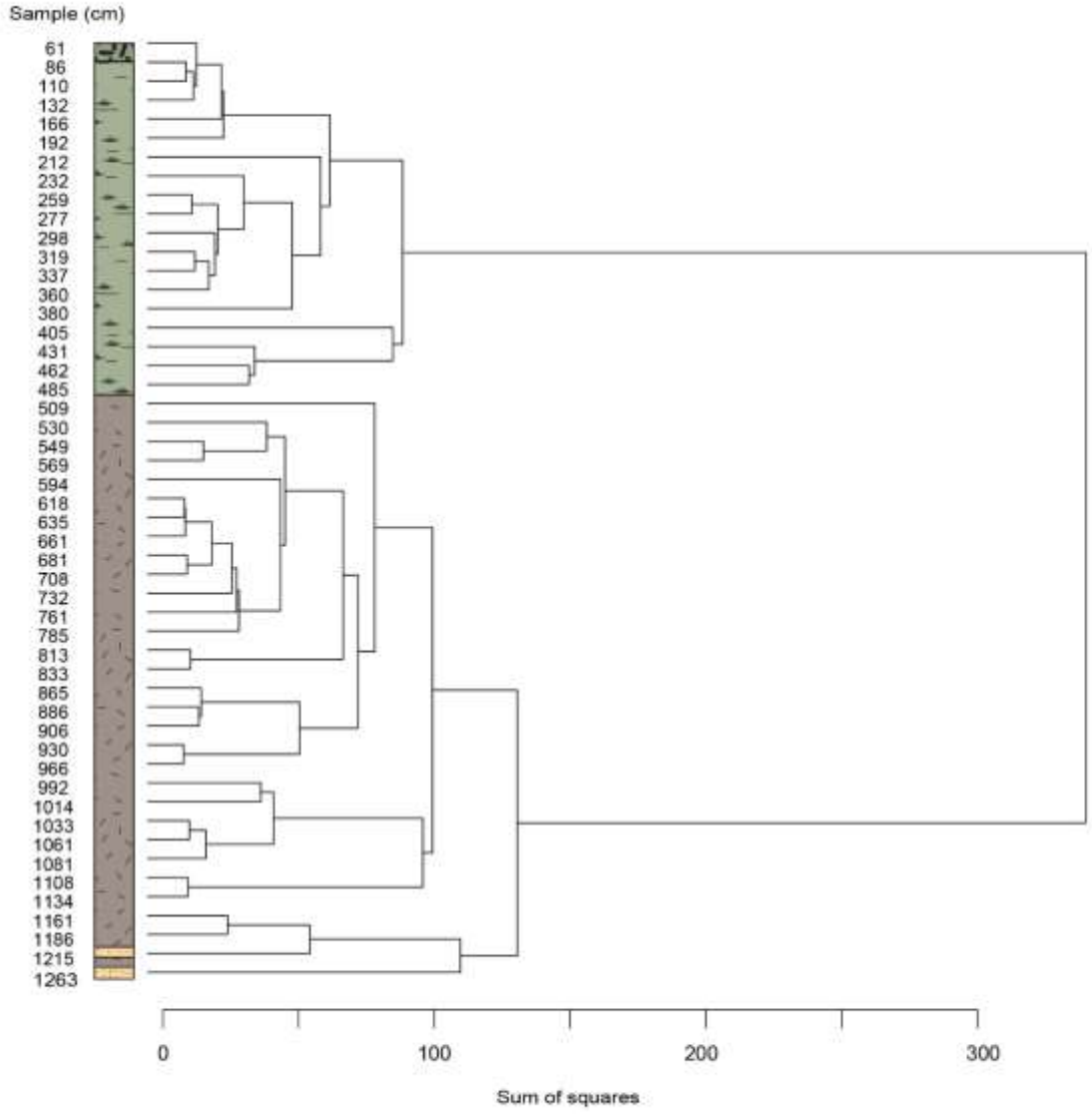

Figure S3: Constrained incremental sum of squares (CONISS) of geochemical data (TOC, TN, $\delta^{13}C$, $\delta^{15}N$). Dendrogram denotes zones according to heirarchical clustering of data based on similarities of samples. Sediment lithology is used in accordance with the CONISS analysis to determine the major periods of change in the record.

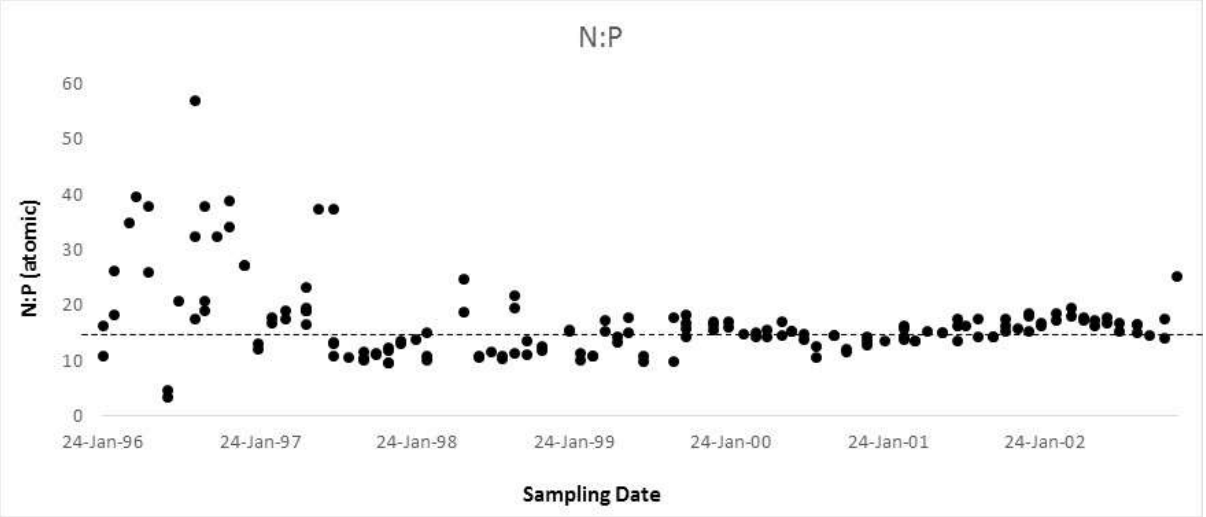

Figure S4: Nitrogen and Phosphorus data from Brown Lake NSI from the period January 1996 to November 2002. Dashed line indicates Redfield ratio of 16:1 N:P as a threshold of N limitation. Data from Mosisch & Arthington (2001).

Table S3. Modern plant and algae samples from NSI

Site	Species	δ13C	%C	%N	C:N
Welsby Lagoon	*Leperonia articulata*	-26.2	47.0	0.6	81.7
Blue Lake	*Leperonia articulata*	-26.8	42.5	0.7	62.8
Swallow Lagoon	*Leperonia articulata*	-27.4	46.1	0.7	72.8
Welsby Lagoon	Baumea spp.	-26.7	44.7	0.6	116.5
Swallow Lagoon	Baumea spp.	-28.0	45.1	0.5	146.2
Blue Lake	Gahnia spp.	-28.4	44.3	0.8	52.1
Welsby Lagoon	*Cycnogeton procerus*	-24.6	38.0	2.2	19.4
Blue Lake	Triglochin spp.	-23.0	37.8	2.1	18.0
Blue Lake	Eleocharis spp.	-29.4	40.2	0.9	44.2
Blue Lake	Casuarina	-30.4	48.3	1.1	44.2
Blue Lake	Eucalyptus	-31.0	20.4	0.7	29.4
Blue Lake	Banksia	-31.6	49.0	0.8	58.1
Blue Lake	Lake Surface	-29.8	42.1	0.8	51.5
Blue Lake	Soil sample	-28.4	2.7	0.1	22.3
Blue Lake	Cyanobacteria	-29.8	36.7	1.9	19.1
Blue Lake	*Hapalosiphon spp.*	-31.7	38.3	2.1	18.1
Welsby Lagoon	Cyanobacteria	-27.2	45.9	2.5	18.6
Amity Swamp	Cyanobacteria	-29.3	50.8	1.1	46.8
Swallow Lagoon	Plankton	-27.9	57.0	2.6	22.0

Group totals	δ13C	%C	%N	C/N
Aquatic Algae	-29.1	45.7	2.1	24.8
Submerged Plants	-26.2	39.0	1.5	31.1
Terrestrial Plants	-31.0	39.2	0.9	43.9
Emergent Plants	-26.8	43.2	1.0	68.6

Supplementary References

Aitken, M. J., 1985. Thermoluminescence dating. Academic press

Arnold, L. J., Bailey, R. M. ,Tucker, G. E., 2007. Statistical treatment of fluvial dose distributions from southern Colorado arroyo deposits. *Quaternary Geochronology*, 2(1): 162-167

Arnold, L. J., Roberts, R. G., Galbraith, R. F., et al., 2009. A revised burial dose estimation procedure for optical dating of youngand modern-age sediments. *Quaternary Geochronology*, 4(4): 306-325

Arnold, L. J., Roberts, R. G., Galbraith, R. F., et al., 2009. A revised burial dose estimation procedure for optical dating of young and modern-age sediments. *Quaternary Geochronology*, 4(4): 306-325

Bailey, R. M. ,Arnold, L. J., 2006. Statistical modelling of single grain quartz De distributions and an assessment of procedures for estimating burial dose. *Quaternary Science Reviews*, 25(19-20): 2475-2502

Brennan, B. J., 2003. Beta doses to spherical grains. *Radiation Measurements*, 37(4): 299-303

Duller, G. A. T., 2003. Distinguishing quartz and feldspar in single grain luminescence measurements. *Radiation measurements*, 37(2): 161-165

Galbraith, R. F., Roberts, R. G., Laslett, G. M., et al., 1999. Optical dating of single and multiple grains of quartz from Jinmium Rock Shelter, Northern Australia: part I, experimental design and statistical models. *Archaeometry*, 41(2): 339-364

Guérin, G., Mercier, N. ,Adamiec, G., 2011. Dose-rate conversion factors: update. *Ancient TL*, 29(1): 5-8

Mejdahl, V., 1979. Thermoluminescence dating: Beta-dose attenuation in quartz grains. *Archaeometry*, 21(1): 61-72

Barr, C., Tibby, J., Moss, P.T., Halverson, G.P., Marshall, J.C., McGregor, G.B., & Stirling, E. (2017) A 25,000-year record of environmental change from Welsby Lagoon, North Stradbroke Island, in the Australian subtropics. *Quaternary International*, **449**, 106–118.

Mosisch, T.D. & Arthington, A.H. (2001) Polycyclic aromatic hydrocarbon residues in the sediments of a dune lake as a result of power boating. *Lakes and Reservoirs: Research and Management*, **6**, 21–32.

Moss, P.T., Tibby, J., Petherick, L., McGowan, H., & Barr, C. (2013) Late Quaternary vegetation history of North Stradbroke Island, Queensland, eastern Australia. *Quaternary Science Reviews*, **74**, 257–272.

Olley, J. M., Pietsch, T. ,Roberts, R. G., 2004. Optical dating of Holocene sediments from a variety of geomorphic settings using single grains of quartz. *Geomorphology*, 60(3-4): 337-358

Prescott, J. R. ,Hutton, J. T., 1994. Cosmic ray contributions to dose rates for luminescence and ESR dating: large depths and long-term time variations. *Radiation measurements*, 23(2): 497-500

Rees-Jones, J., 1995. Optical dating of young sediments using fine-grain quartz. *Ancient TL*, 13(2): 9-14

Rees-Jones, J. ,Tite, M. S., 1997. Optical Dating Results for British Archaeological Sediments. *Archaeometry*, 39(1): 177-187